

10
3-24-97 JS(1)

1497052275


SANDIA REPORT

SAND97-8212 • UC-702
Unlimited Release
Printed March 1997

Hydrothermal Oxidation of Navy Shipboard Excess Hazardous Materials

C. A. LaJeunesse, B. L. Haroldsen, S. F. Rice, B. G. Brown

MASTER



Prepared by:
Sandia National Laboratories
Albuquerque, New Mexico 87185 and Livermore, California 94551
for the United States Department of Energy
under Contract DE-AC04-94AL85000

Approved for public release; distribution is unlimited.



Issued by Sandia National Laboratories, operated for the United States Department of Energy by Sandia Corporation.

NOTICE: This report was prepared as an account of work sponsored by an agency of the United States Government. Neither the United States Government nor any agency thereof, nor any of their employees, nor any of the contractors, subcontractors, or their employees, makes any warranty, express or implied, or assumes any legal liability or responsibility for the accuracy, completeness, or usefulness of any information, apparatus, product, or process disclosed, or represents that its use would not infringe privately owned rights. Reference herein to any specific commercial product, process, or service by trade name, trademark, manufacturer, or otherwise, does not necessarily constitute or imply its endorsement, recommendation, or favoring by the United States Government, any agency thereof or any of their contractors or subcontractors. The views and opinions expressed herein do not necessarily state or reflect those of the United States Government, any agency thereof, or any of their contractors or subcontractors.

This report has been reproduced from the best available copy.

Available to DOE and DOE contractors from:

Office of Scientific and Technical Information
P.O. Box 62
Oak Ridge TN 37831

Prices available from (615) 576-8401, FTS 626-8401.

Available to the public from:

National Technical Information Service
U.S. Department of Commerce
5285 Port Royal Rd.
Springfield, VA 22161

DISCLAIMER

**Portions of this document may be illegible
in electronic image products. Images are
produced from the best available original
document.**

HYDROTHERMAL OXIDATION OF NAVY SHIPBOARD EXCESS HAZARDOUS MATERIALS*

C. A. LaJeunesse, B. L. Haroldsen, S. F. Rice, and B. G. Brown
Sandia National Laboratories
Livermore, California

ABSTRACT

This study demonstrated effective destruction, using a novel supercritical water oxidation reactor, of oil, jet fuel, and hydraulic fluid, common excess hazardous materials found on-board Navy vessels. This reactor uses an advanced injector design to mix the hazardous compounds with water, oxidizer, and a supplementary fuel and it uses a transpiring wall to protect the surface of the reactor from corrosion and salt deposition. Our program was divided into four parts. First, basic chemical kinetic data were generated in a simple, tubular-configured reactor for short reaction times (<1 second) and long reaction times (>5 seconds) as a function of temperature. Second, using the data, an engineering model was developed for the more complicated industrial reactor mentioned above. Third, the three hazardous materials were destroyed in a quarter-scale version of the industrial reactor. Finally, the test data were compared with the model. The model and the experimental results for the quarter-scale reactor are described and compared in this report. A companion report discusses the first part of the program to generate basic chemical kinetic data.

The injector and reactor worked as expected. The oxidation reaction with the supplementary fuel was initiated between 400 °C and 450 °C. The released energy raised the reactor temperature to greater than 600 °C. At that temperature, the hazardous materials were efficiently destroyed in less than five seconds. The model shows good agreement with the test data and has proven to be a useful tool in designing the system and understanding the test results.

* This work is part of a project directed by the Defense Advanced Research Projects Agency (DARPA), to develop a supercritical water oxidation reactor to destroy excess hazardous materials on-board Navy vessels.

Table of Contents

Introduction.....	7
1.1 Background.....	7
1.2 Transpiring Wall Reactor.....	8
1.3 Sandia's Responsibilities.....	8
Experimental Setup.....	9
2.1 Transpiring Wall Reactor/Injector Description.....	9
2.2 Scaling.....	9
2.3 EER System Design.....	10
2.4 Experimental Procedure.....	11
2.5 Temperature Profiles.....	11
Results and Discussion.....	11
3.1 Overview.....	11
3.2 Tests to Initiate Reaction.....	12
3.3 Test to Destroy Methanol and Jet Fuel.....	14
3.4 Tests with Salt.....	15
3.5 Tests to Destroy Oil.....	16
3.6 Test to Destroy Hydraulic Fluid.....	18
3.7 Implications for Full Scale System.....	18
Model.....	18
4.1 Introduction.....	18
4.2 Graphical User Interface.....	19
4.3 Model Development.....	19
4.4 Comparison with Data.....	20
Summary and Conclusions.....	21
References.....	21-22

List of Figures

Figure 1.	Conceptual operation of the transpiring wall reactor showing the various fluid streams.....	23
Figure 2.	The test reactor is a 1/4 scale version of the prototype	23
Figure 3.	Cross-sectional illustration of the stream entering the reactor region from the injector	24
Figure 4a.	Schematic of Sandia's Engineering Evaluation Reactor (EER) configured to test the transpiring wall reactor.....	25
Figure 4b.	Schematic showing location of thermocouples in the top reactor section to measure fluid temperatures.....	25
Figure 5.	Process temperature, TC, TIC, and TOC (sixth test)	28
Figure 6.	Process temperature, TC, TIC, and TOC (seventh test).....	28
Figure 7.	Process temperature, TC, TIC, and TOC (eighth test).....	29
Figure 8.	Conductivity data/salt balance (ninth test)	29
Figure 9.	Salt Deposition photo (ninth test).....	30
Figure 10.	Salt Deposition photo (ninth test).....	30
Figure 11.	Process temperature, TC, TIC, and TOC (tenth test)	31
Figure 12.	Process temperature and differential pressure (eleventh test).....	31
Figure 13.	Process temperature and EHM orifice pressure differential (twelfth test).....	32
Figure 14.	Graphical User Interface for code	33
Figure 15.	Calculated temperature profile, DRE, and residence time for the destruction of JP-5	34
Figure 16.	Calculated temperature profile, DRE, and residence time for the destruction of oil.....	35
Figure 17.	Calculated temperature profile, DREm and residence time for destruction of hydraulic fluid.....	36
Appendix A.	Code.....	37-46

List of Tables

Table 1. Test Summary	29
Table 2. Test conditions for sixth test (NPA initiation).....	29
Table 3. Design conditions	29
Table 4. Test conditions for seventh test at 295 minutes.....	29
Table 5. Test conditions for eighth test	29
Table 6. Test conditions for ninth test.....	29
Table 7. Input conditions to model	29
Table 8. Initial test conditions for tenth test	29
Table 9. Operating conditions at the end of the tenth test	29
Table 10. Test conditions at 90 minutes for the eleventh test	30
Table 11. Test conditions for test 12.....	30

Hydrothermal Oxidation of Navy Shipboard Excess Hazardous Materials

C.A. LaJeunesse, B.L. Haroldsen, S. F. Rice, and B. G. Brown
Sandia National Laboratories
Livermore, California

NOMENCLATURE

A	inside cross-sectional area
cp	heat capacity
C	concentration
d	diameter
dx	differential positional element
dt	differential time element
f	fraction of organic converted
h	enthalpy
j	j th element
\dot{m}	flow rate
N	organic
T	temperature
V	velocity
x	reactor position
α	void fraction
λ	heat of combustion
ρ	density
η	effectiveness ratio

Subscripts

a	air
c	core/center
lhs	left-hand-side
NPA	1-propanol
p	platelet
rhs	right-hand-side
t	transpiration
w	waste/water/wall

INTRODUCTION

1.1 BACKGROUND: Supercritical Water Oxidation (SCWO) is a technically viable waste treatment method for many organic compounds including excess hazardous materials (EHM) on-board Navy vessels [1]. SCWO is being considered by private industry, the Department of Defense (DoD), and the Department of Energy (DOE), to destroy chemical waste, chemical warfare agents, and obsolete munitions; amongst the most difficult compositions of hazardous wastes to destroy.

In 1994, the Advanced Research Projects Agency (ARPA), an agency of the United States Government, issued a Broadcast Agency

Announcement (BAA) to meet the Navy need of eliminating the discharge of untreated hazardous material in response to advancing international regulations. This BAA was targeted for development and testing of a supercritical water oxidation reactor to be installed on-board Navy vessels to treat excess hazardous materials. These chemicals range from contaminated diesel and jet fuel to hydraulic fluids and lubricating oils.

Sandia National Laboratories was invited by Foster Wheeler Development Corporation (FWDC) to join the FWDC team in response to the BAA. ARPA awarded the FWDC team, and two competing teams, contracts to develop SCWO reactors.

Sandia's association with FWDC on SCWO began two years prior to this when FWDC was the successful bidder on a Request for Quotes that Sandia issued to design and build a SCWO prototype plant for the Army. The prototype plant is currently being built at Pine Bluff Arsenal, Arkansas. The plant, with a capacity of 80 pounds of waste per hour, will be used to destroy hazardous colored smokes and dyes [3].

Sandia began an applied research and development program in SCWO in 1987 and has four on-site SCWO reactors. During FY92, we destroyed representative Navy wastes, including industrial chemicals, for the U. S. Naval Civil Engineering Laboratory (NCEL) in a tubular-configured Inconel 625 reactor to determine appropriate temperature ranges and performance problems for SCWO of methanol, ethylene glycol, phenol, methyl ethyl ketone (2-butanone), acetic acid, methylene chloride (CH₂Cl₂), 1,1,1 Trichlorethane (TCA), latex paint, herbicide, and motor oil [1, 2].

Simultaneously, Sandia conducted a research program to determine the feasibility of using SCWO to destroy the hazardous colored smokes and dyes for the Army [3, 4, 5, 8, 9].

1.2 THE TRANSPIRING WALL REACTOR:

The two major recurring problems with the application of SCWO, identified in these and other studies, are 1) salts, soluble at ambient conditions, precipitate into a second phase at supercritical conditions, deposit on reactor walls, and eventually plug the reactor thereby interfering in the processing of the organic constituent, and 2) the processing of the organic constituent produces acids which leach reactor material into the effluent stream. Salts are bound to the organic component and form during the conversion to CO₂. Other heteroatoms bound to the organic component, such as sulfur or chlorine, form acids and, in the absence of a balanced cation such as sodium, leach the reactor material. Leaching of material is a general form of corrosion [6, 7, 8].

GenCorp, Aerojet, part of the FWDC team, has developed a concept to mitigate or eliminate both salt deposition and corrosion by forming a protective boundary layer of pure water along the reactor wall. Aerojet has successfully applied this transpiring wall concept to aerospace applications such as cooling rocket nozzles and nose cones [11].

The transpiring wall reactor concept is illustrated in Figure 1. An inner liner, called a platelet, distributes water uniformly to small transpiration pores along the inner surface through a complex system of internal manifolding and metering channels. The boundary layer forms a protective barrier constraining the reaction zone to a central core region. The volume between the outer wall of the reactor and the platelet forms a plenum from which water is fed into the platelet. Because it is based on Aerojet's platelet technology, the transpiring wall reactor is often referred to as the platelet reactor [14, 15].

1.3 SANDIA'S RESPONSIBILITIES: One of the four SCWO reactors at Sandia is the Engineering Evaluation Reactor (EER), a multipurpose facility that was reconfigured from a tubular reactor to a test bed for the transpiring wall reactor. It was used extensively to generate data on salt deposition and dye destruction rate efficiency (DRE) for the Army waste [9,10] and to destroy ammonium picrate, a high-explosive, for the Naval Surface Warfare Center in Crane, Indiana [12]. It can be remotely operated, can be used to test hazardous materials for destruction by SCWO, and uses state-of-the-art techniques for data acquisition and control.

Sandia proposed to experimentally demonstrate the efficacy of the Aerojet/Foster Wheeler/Sandia reactor design by destroying specific Navy EHM streams in the EER. Two major variations in the design of the reactor from previous tests for the Army were implemented: 1) For the Navy design, it was necessary to use air as the oxidant. The tests for the Army used hydrogen peroxide (H₂O₂) as the oxidant. The H₂O₂ thermally decomposed before entering the reactor, producing a stream of oxygen dissolved in water. Using air eliminates the need to carry an oxidant on-board ship which is logistically impractical. 2) An injector was designed by Aerojet and incorporated by Sandia into the EER to mix the fluid streams entering the reactor. As the EHM stream enters the reactor, it must be heated from subcritical temperature to supercritical temperature for rapid oxidation. In the tests for the Army, this was done by adding 600 °C (1112 °F) supercritical water through radial injection holes at the top of the platelet [9]. The new injector, described in detail later, allowed the use of a supplementary fuel to reduce the demand for heating water. It also directed all fluid streams nearly parallel to the axis of the reactor to reduce turbulent disturbance of the protective boundary layer. Significant effort was expended in the development of subsystems to support these two new components and in testing of the injector. This is expanded on in the body of the report.

The test plan was divided into two phases. Phase I Tasks were completed in our Supercritical Fluids Reactor [13], a tubular configured reactor¹. Phase I tasks were intended to obtain data during the early stages of oxidation and to obtain total reaction behavior by running reactions to near completion. Global heat release data were also developed from these tests. Total reaction data and early reaction rates are key parameters needed to determine the platelet reactor operational configuration and design. These data were used as input to a code that was developed as part of this work to allow experiments to be designed for the EER and data to be interpreted from it.

Phase II tasks were intended to demonstrate the "efficacy" of the platelet reactor. Specifically, tests were done to initiate and sustain the reaction with air, and to destroy three Navy EHM surrogates: JP-5 jet fuel, H-537 hydraulic

¹ Also called the Materials Evaluation Reactor (MER) in some of our papers.

fluid, and Delo 400 Chevron oil. All three materials are various compositions of hydrocarbons with selected additives. The compositions are described in [13]. Also described in [13] are the results from Phase I testing. The results from Phase II testing are described in this paper. The model that was developed to understand and guide Phase II testing is also documented here.

EXPERIMENTAL SETUP

2.1 TRANSPIRING WALL REACTOR /INJECTOR DESCRIPTION: The test reactor, designed and fabricated by Aerojet, is a 1/4 scale version of the reactor to be installed on-board ship. The configuration of the 1/4 scale reactor and the EER system is described in [9] and given limited treatment here.

Figure 2 shows the 1/4 scale design. The reactor has an inside diameter of 2.8 cm (1.1 inches), an outside diameter of 6.35 cm (2.5 inches), and a total length of 91.4 cm (36 inches). The outer wall of the reactor is made of Inconel 625. An inner liner of the reactor, the platelet, distributes water uniformly to the small transpiration pores along the inner surface. The top platelet section is made of Inconel 600 while the bottom platelet section is 316 SS; it was reused from the Army program, where 316 SS was the design material, to reduce cost.

The volume between the outer wall and the platelet forms a plenum from which water is fed into the platelet. It is fed through two lines, each typically supplying up to 5.25 gm/s (5 gallons per hour) of water at temperatures of 450 °C (842 °F) or less. At this flow rate and temperature, the pressure drop through the internal channels is about 13.8 bar (200 psi) in the bottom platelet, and 17.2 bar (250 psi) in the top platelet, due to differing metering designs.

Five inlets are located in the multi-stream injector at the head of the reactor. A stream of supplementary fuel is mixed with a stream of hot, supercritical water, then with a stream of air, causing it to react rapidly. This acts as a "chemical spark plug" in the center of the reactor. The released energy heats the other streams to the required reaction temperature. Figure 3 shows the pattern for the inlet streams into the reactor region (exiting from the injector) Within the injector, the air is split into two streams, one that mixes with the hot water and supplementary fuel streams, and the second that

mixes with the waste or EHM stream. This is designed such that, if \dot{m}_a is the total air flow rate entering the injector, then $0.25 \dot{m}_a$ mixes with the hot water stream and "fuel" and $0.75 \dot{m}_a$ mixes with the EHM.

The injector's five streams, entering at different temperatures, are: 1) the hot water stream, used to bring the air and fuel to high temperature, entering at \dot{m}_h gm/s and T_h , 2) the injector face protection stream, used to protect the face of the injector from corrosion and salt deposition, entering at \dot{m}_d gm/s and T_d , 3) the fuel stream, used to initiate the reaction, entering at \dot{m}_{NPA} gm/s and T_{NPA} , 4) the air stream, used to convert the EHM to CO₂ and water, entering at \dot{m}_a gm/s and T_a , and 5) the EHM stream, entering at \dot{m}_w gm/s and T_w . The actual quantities are varied during the tests. The typical operating pressure is 240 bar (3500 psi).

The supplementary fuel for the "chemical spark plug" on these tests was n-propyl alcohol (NPA). The choice of NPA and the possible use of JP-5 as an alternative is discussed in [13]. The theoretical mixing temperature of the three core streams $0.25 \dot{m}_a$, \dot{m}_h , \dot{m}_{NPA} in excess of 500 °C (932 °F), was sufficient to initiate the release of the chemical energy of the NPA and begin the destruction of the EHMs. The theoretical mixing temperature depends on actual input conditions to the injector and can be calculated using the code described in this report. Demonstration of this "chemical spark plug" was a central goal of Sandia's program and was accomplished as described below.

2.2 SCALING: Although the test reactor is basically a 1/4 scale model, two aspects of this reactor should be discussed. First, the length of the test reactor does not provide sufficient residence time to destroy the EHM at a destruction rate efficiency (DRE) greater than 98%. The ability of SCWO to destroy the Navy EHM at DREs greater than this was demonstrated in Phase I testing on the MER [13] and in the contract with NCEL [1]. Second, the ratio of EHM to transpiration fluid does not scale linearly with reactor diameter and is considerably smaller in the laboratory scale model than in the analogous full scale reactor. Geometrically, the spacing and pore pattern is the same in the 1/4 scale model as the full-scale reactor. Hence, the flow rate of transpiration fluid, \dot{m}_p , scales with the surface area which is proportional to the diameter:

$$\dot{m}_p \propto d.$$

However, core flow, \dot{m}_c , is proportional to cross-sectional area which scales as the diameter squared:

$$\dot{m}_c \propto d^2.$$

If the diameter of the test reactor is one-quarter that of the full-scale reactor, the total transpiration or platelet flowrate of the full scale unit is then four times the test case, but the core flow rate is 16 times. Hence, it is not possible to maintain strict geometric similitude.

To establish similitude between the test reactor and the Navy reactor, the platelet wall protection effectiveness ratio, η , is used as the dimensionless parameter. The wall protection effectiveness ratio is defined as:

$$\eta = (C_c - C_w) / (C_c - C_i)$$

where C is the calculated concentration of EHM and the subscripts refer to the location in the center of the reactor (c), at the surface of the reactor (w), and in the transpiration flow (i). C_i , in this case, is zero because pure water is used to protect the platelet. At an effectiveness ratio of one, salts and acids will not be in contact with the wall.

The effectiveness ratio is a calculated number that is used to establish similitude between the quarter-scale and full-scale systems. It is not a measurement of how "effective" the platelet is at preventing salt deposition or corrosion. Once appropriate flow conditions are determined, the effectiveness ratio is used to select analogous operating conditions in the full scale system. Like other dimensionless numbers used in fluid mechanics and heat transfer, the effectiveness ratio is calculated from the geometry, temperature, pressure, flow rates, and thermodynamic properties of the fluids. The calculation, however, is complex and is done with Aerojet's computer design code [14].

In choosing the effectiveness ratio as the scaling parameter, similitude of other fluid dynamic properties, such as Reynolds number, and geometry, as discussed previously, are not maintained. This is an inherent problem in scale model testing. The implication on test results has not been further considered. This discussion is documented here for completeness.

2.3 EER SYSTEM DESIGN: Figure 4a shows a schematic of the EER with the transpiring wall reactor. The EER is a second generation, laboratory scale reactor system designed specifically for evaluating engineering aspects of SCWO technology. Its modular design facilitates different test configurations and its computer based control system allows maximum flexibility in operating conditions. It has a maximum operating temperature of 650 °C (1202 °F) at an operating pressure of 345 bar (5000 psi). As mentioned earlier, a detailed description of the EER is given in [9].

Separate pumps supply the EHM, the fuel, the injector face protection water, the transpiration water, the injection-heating water, and the injection-cooling water at pressures up to 345 bar (5000 psi). Air is supplied by a 2 stage compressor. All tests were done at about 240 bar (3500 psi). The EHM and fuel pumps supply water during reactor startup and shutdown. This is accomplished by remotely switching the feed to the pump. The EHM pump may supply a salt solution or an organic compound solution during operation. The lines entering and leaving the reactor are 1.4 cm (9/16-inch) outside diameter (OD), and 0.48 cm (3/16-inch) inside diameter (ID) Inconel 625 tubing. Pressure transducers and thermocouples are installed in "T-unions" to measure fluid pressure and temperature at various locations. Pressure measurements are not possible within the reactor due to the double wall geometry. The fluid streams are heated with cable heaters wrapped around the tubing.

The effluent is cooled in a counterflow heat exchanger and is discharged through a liquid back pressure regulator that controls the pressure in the system. A small fraction of the low pressure effluent stream can be diverted to a fraction collector for post-test chemical analysis. The remaining effluent flows through on-line conductivity and pH meters. An on-line spectrometer also collects absorption spectra from which various compounds in the effluent can be detected. Samples are analyzed on-line for total carbon (TC), total inorganic carbon (TIC), and total organic carbon (TOC).

The reactor system is controlled remotely through a graphical user interface by LabVIEW on a Macintosh Quadra 950. The interface also logs the reactor condition throughout the test.

2.4 EXPERIMENTAL PROCEDURE: The detailed procedure is test specific and is described further in the results and discussion section. However, the following general procedures are followed:

1. Power and control air are supplied to the EER.
2. Computer control is initiated.
3. Pumps are actuated to establish the flow of water to all lines feeding the reactor/injector.
4. Pressure is increased by actuating the back-pressure regulator.
5. The input streams to the reactor/injector are gradually heated to design temperature.
6. Air is introduced into the reactor/injector.
7. After stabilizing the temperature, NPA is introduced.
8. If the NPA reacts, this increases the process temperature. After stabilization, the EHM or salt solution is introduced.
9. After collecting data, any EHM or salt solution feed is switched to pure water. The reactor is flushed, depressurized, and allowed to equilibrate over-night. If an inspection of deposits within the reactor is warranted, the reactor is not flushed.

Due to the emphasis on testing the reactor/injector for performance, and the number of input variables, many adjustments are made during a single test.

2.5 TEMPERATURE PROFILES: Figure 4b shows the location of thermocouples in the injector and top reactor regions. The thermocouples measuring the transpiration fluid in the plenum volume are duplicated on the lower platelet section. Another thermocouple measures the effluent temperature exiting the reactor. Not all thermocouples are active on every test. Temperatures inside the reactor are measured by 0.16 cm (1/16 inch) Inconel 600, ungrounded, sheathed thermocouples (TCs) inserted through the injector to various depths. For most tests, the thermocouples were inserted 2.5 cm (1 inch), 7.5 cm (3 inches), and 12.5 cm (5 inches), measured from the internal face of the injector. For some tests, the TCs were inserted as far as 25 cm (10 inches).

The remaining temperatures are inferred by a uniaxial model developed from continuity and energy principles, that includes a model for NPA and EHM energy release, and air transport. This model is used to calculate residence time and is described at the end of the report.

During the discussion, the terms "process" temperature and "reactor" temperature refer to the recorded temperature at either the 1, 3, or, 5 inch location. When differentiation is necessary, the location is clearly identified.

RESULTS AND DISCUSSION

3.1 OVERVIEW: Results are summarized in Table 1 and discussed in detail in this section.

After installing the Aerojet injector, the air subsystem, several support subsystems, and trouble-shooting the entire system, tests were first conducted to initiate a reaction with the NPA. The first seven tests concentrated on initiating this reaction. Several problems that are described below occurred, and it was not until the sixth test that success was achieved.

After initiating a reaction with the NPA, a simulated EHM, methanol, was successfully destroyed. We then destroyed the first EHM of interest to the Navy, the JP-5 jet fuel. This was also successful. DRE was in excess of 98.5% with a calculated residence time of less than 4.6 seconds.

On the ninth test, an attempt was made to quantify salt transport through the reactor with the new injector. Less than 100% of the salt was transported through the reactor. The system was depressurized with the salt "frozen" in place for post-test inspection. The inspection revealed deposition at the interior surface of the injector.

Oil was destroyed in the next two tests. These tests were successful and interesting. Most notably, at one point pure oil (100% oil at the injector orifice) was injected into the reactor and the reaction was self-sustaining without NPA being injected into the reactor. The process temperature was over 650 °C (1202 °F) and stable. DRE was again over 98.5%.

As a final test, the hydraulic fluid was destroyed. Process temperature was in excess of 640 °C (1184 °F). It was not possible to determine DRE accurately due to unsteady flow conditions.

3.2 TESTS TO INITIATE REACTION: The intent of these tests was to demonstrate the concept of mixing NPA with hot water and air to release the chemical energy of the NPA. The released energy is needed to increase the temperature of the EHM stream to process temperatures capable of initiating the conversion of EHM to CO₂. Any problems that were experienced are described so that they will not be repeated in the Navy system.

The injector plugged on the first test and required extensive work at Aerojet to clean out the channels and the 0.2 mm (0.008 inch) orifices. Among other debris, small black particulate had plugged the orifice. An investigation into the cause of the particles revealed that the packing of the pump feeding this line had minutely eroded. All lines to the injector were protected from particulate by in-line filters, but the filter had been placed in the inlet line, upstream of the pump. High-pressure pumps are built with check-valves that prematurely erode if particulate is allowed to pass-through the orifices. Placement of a filter before a high-pressure pump is standard design practice to prevent premature check-valve failure. We felt that this would also protect the injector. It did not due to the erosion of the pump packing. Other material removed from the injector indicated that the tubing between the pumps and the reactor was not sufficiently clean.

After this incident, the filtration system was redesigned. Dual filters -- a 60 micron filter followed by a 7 micron filter -- were placed downstream of all high-pressure pumps. Filters were located as close as possible to the injector. However, some input lines (to the injector) were heated in excess of 400 °C (752 °F). At these temperatures, oxidation of the 316 SS filters² was a concern. Filters on the EHM and fuel lines, where concern of plugging was greatest, were placed within a few inches of the injector. On the other streams, which were heated to greater than 400 °C (752 °F), the filters were placed before the heated section but after the pump. Inspection of the filters from the fuel line, after use at elevated temperature, has shown discoloration of the filters from oxidation, but no evidence that it led to plugging. In addition to improved filtration, the reactor input-lines were cleaned by repeatedly rinsing the lines with water and "blowing-down" the lines with nitrogen.

² Filter materials other than 316 SS may be available but were not tried.

Water samples from each line showed no particles in excess of 100 microns at the inlet to the injector. These steps proved to be successful.

Five injector initiation tests were attempted before success was achieved. Failure of several components unrelated to the injector, such as air flowmeters and temperature controllers, terminated most tests. Termination of the fourth test, however, was caused by a pressure rise upstream of the injector, as if the injector had plugged again. The differential pressure across the injector on the NPA line gradually escalated over a period of one hour from a pressure of 6 bar to 41 bar (80 psi to 600 psi). The fluid entering the injector was at a temperature of 400 °C (752 °F). The reason for the pressure increase was not discovered. No pluggage was observed the next day when the injector was back-flowed at low pressure and ambient temperature.

Test 6 was the first successful test. The conditions of the test are shown in Table 2; test results are shown in Figure 5. To insure reaction with the NPA, all fluid streams were heated to higher temperatures than design conditions (see Table 3) and the flow rate of heating water was increased. The flow meter for the heating water appeared to read incorrectly so the exact flow is not known, but it was between 2 and 3 gm/s (1.9 and 2.9 gallons/hour). As shown in Table 3, the design value is 1.1 gm/s (1.05 gallons per hour). The flow of platelet water was reduced to about 3 gm/s (2.9 gallons per hour) in each section to reduce the demand on the effluent chiller. The heating water and injector face protection water were both at 590 °C (1094 °F), measured inside of the injector (temperatures entering the injector were hotter). The NPA and EHM streams were both at 390 °C (734 °F). The platelet protection water was about 600 °C (1112 °F) entering the plenum volume, but was only 460 °C (860 °F) on the opposite side.

Water, with no organic constituent, was used as the EHM stream (only injector initiation was being tested). Water was used for the NPA stream during the heat-up phase and then switched to a 15 wt% solution of NPA once the test conditions were reached. Thermocouples measured the process temperature at one, three, and five inches below the injector. On-line TOC analysis provided near-real-time feedback on the destruction of the NPA. After introduction of the NPA, the temperature one inch below the injector (see Figure 4b) climbed from 470 °C to

520 °C (878 °F to 968 °F). Five inches down, it increased from 475 °C to 535 °C (887 °F to 995 °F). During the test, TOC was about 20 ppm compared with a calculated value of 1600 ppm with no reaction³. The NPA clearly reacted and released substantial heat in the top portion of the reactor.

The temperatures of the various inlet streams were then gradually reduced to design operating conditions. During this time, the NPA solution continued to flow through the reactor. Heating water, injector face protection water, and EHM steam temperatures were reduced to 570 °C, 450 °C, and 320 °C (1058 °F, 842 °F, and 608 °F), respectively. Heating water flow rate was also reduced. The combined effect was to reduce the temperature five inches below the injector from 535 °C to 400 °C (995 °F to 752 °F). The TOC measurements climbed slowly to 70 ppm. At these conditions, the temperature increase between the one and five inch thermocouples was only 7 °C (13 °F). After switching the NPA stream to water, the temperature at five inches decreased by 17 °C (31 °F). Apparently, the NPA continued to react at the lower temperature, but at a slower rate, distributing the release of chemical energy along the length of the reactor instead of the top portion.

Although the total air flow on this test was enough for complete oxidation of the NPA, the injector supplied only a fraction of it into the hot "spark plug" region. The rest was mixed with the EHM stream (water in this case) and mixed with the NPA further down the reactor. Consequently, the reaction in the "spark plug" region may have been limited by lack of oxidizer rather than chemical kinetics.

For test 7, the air flow rate was increased to guarantee that the NPA had excess oxidant delivered to it in the spark plug region. The conditions for this test at 295 minutes, when the NPA line was switched from water to NPA, are shown in Table 4; test results are shown in Figure 6. Initially, the flow rates and temperatures were at the nominal design conditions producing a reactor temperature of about 350 °C (662 °F). The NPA flow was

turned on, but little or no reaction occurred; TOC was 675 ppm and the reactor temperature remained constant. Heating water flow rate was then increased to 1.9 gm/sec (1.8 gallons per hour). Reactor temperatures, then climbed 15 °C (27 °F) as TOC slowly declined but remained above 400 ppm. Injector face protection water, at 450 °C (842 °F) and greater than the bulk reactor temperature, was then discontinued. Temperatures at one and three inches below the injector decreased 10 °C (18 °F). However, the process temperature at five inches increased a few degrees, suggesting some heat release from the NPA.

The EHM flow, devoid of organic, was then shut-off. With its inlet temperature of 300 °C (572 °F), it had a large cooling effect when mixed with the other streams entering the injector. Once off, an immediate increase in reactor temperature of 200 °C (360 °F) ensued. About 50 °C (90 °F) of this increase was due to the EHM stream no longer cooling the other streams. The balance of 150 °C (270 °F) resulted from reaction of the NPA. Over the next few minutes, the temperature in the reactor gradually climbed another 50 °C (90 °F) to 625 °C (1157 °F). All three process thermocouples read the same indicating that the NPA reacted in the top 2.5 cm (1 inch) of the reactor. TOC decreased to 25 ppm.

The EHM stream was then resumed. Initially, the pump failed to start against head and flow had to be momentarily increased. With flow resumed, the reactor temperature decreased 200 °C (360 °F), but the NPA continued to react; process temperature was 40 to 60 °C (72 to 108 °F) greater than before the EHM stream was shut off and TOC was 75 ppm. The temperature at five inches was 25 °C (45 °F) greater than at the one or three inch location suggesting that significant heat release occurred between three and five inches.

The sequence was then repeated. First, the air was turned-off stopping the reaction. After starting the air again, the NPA did not react. This was the identical condition and result as the start of the test. To start the reaction, we again discontinued the EHM stream and then reestablished its flow. Results were identical.

To summarize, these tests indicate that the injector performs as intended. NPA initiation occurs in the top portion of the reactor. For initiation, the EHM stream should be introduced after process temperature is established.

³ TOC of 1600 ppm is a calculated value. This is well beyond the calibration range of the TOC analyzer. TOC reading greater than about 500 ppm indicated little or no reaction, but did not accurately reflect the actual TOC concentration.

3.3 TESTS TO DESTROY METHANOL AND JET FUEL: In the next test, methanol and jet fuel were destroyed in the EER. To gain operating experience, methanol was destroyed first. Because it is soluble in water, its concentration in the EHM stream could be controlled more easily.

The system was brought to temperature with water in each stream and no air. NPA was injected by switching the inlet stream to the pump from water to a 15 wt% solution of NPA. The EHM stream was supplied by two pumps to allow a variable concentration of EHM. A high-pressure Milroyal pump supplied water while a high-pressure-liquid-chromatography (HPLC) pump supplied EHM. These two components were mixed at a high-pressure "Tee" prior to being heated. The inlet stream to the HPLC pump could be switched between water and EHM.

With the heating water flowing at the nominal condition of 1 gm/s (0.95 gallons per hour), the temperature was lower than desired; the flow rate was increased to 1.75 gm/s (1.7 gallons per hour). Other conditions are shown in Table 5; test results are shown in Figure 7.

Internal reactor temperature and TOC are shown in Figure 7. At the conditions given in Table 5, the process temperature was 385 °C (725 °F). At 177 minutes, flow of the EHM stream was decreased to 0.1 gm/s (0.095 gallons per hour) by shutting-off the Milroyal pump, leaving only the HPLC pump. The process temperature then increased to 470 °C (878 °F). Forty-five seconds later, the flow in the NPA line was switched from water to NPA solution. Air was not yet introduced; temperature remained constant as TOC increased to 500 ppm. At 196 minutes, air was injected causing an immediate increase in reactor temperature to 580 °C (1076 °F). TOC declined to 40 ppm and inorganic carbon (TIC) increased to 120 ppm indicating carbonic acid production; pH (not shown) declined from 6.4 to 6.1.

After 16 minutes, the EHM flow rate (still pure water) was increased to 1 gm/s (0.95 gallons per hour) by restarting the Milroyal pump. EHM water temperature was 160 °C (320 °F) entering the injector, causing a drop in process temperature to 350 °C (662 °F). TOC climbed to 470 ppm and pH dropped to 5.1 indicating that the NPA may have formed an

acidic compound that was not completely oxidized.

After stabilization of flow and temperatures, at 254 minutes, the HPLC was switched from water to methanol. Simultaneously, the HPLC flow rate was reduced to inject a 5 wt% solution of methanol into the reactor. A 10 to 15 °C (18 to 27 °F) increase in process temperature ensued (see Figure 7). It was due to a change in the flow rate of water and not due to reaction of methanol; it takes several minutes to flush water from the inlet line before organic compound (in this case, methanol) reaches the injector. After 14 minutes, the flow rate of the HPLC was doubled (the calculated solution concentration was then 10 wt%); the temperature decrease at 269 minutes is due to this increase in flow rate. At 270 minutes, the methanol reached the reactor and began to react, raising the process temperature to 450 °C (842 °F). TIC also increased from 100 ppm (NPA only) to 140 ppm (NPA plus methanol).⁴ As methanol reacted, the process temperature continuously increased, with the largest increase occurring five inches from the injector surface.

At 290 minutes, the flow rate from the HPLC was further increased to raise the concentration of methanol at the injector to 15 wt%. At one inch, the temperature increased 150 °C (270 °F) while at five inches, the temperature increased by 100 °C (180 °F). TIC also increased. Despite the large increase in temperature, the temperature of the resultant stream exiting the reactor changed only 5 °C (9 °F). This suggests that the measured temperature increase resulted not only from the increase in the total energy release, but also from a change in the location of the heat release. As the reaction rate increased, the heat release became more concentrated near the top of the reactor where the measurements were made. TOC remained stable at 40 ppm.

At 315 minutes, the feed to the HPLC was changed from methanol to jet fuel and the flow rate from the HPLC was decreased by a factor of two. By halving the flow, the methanol that was still entering the injector was also halved causing a drop in temperature. In the process of

⁴ The TOC analyzer alternately measures total carbon (TC) and then TIC and TOC is determined by subtraction; samples for inorganic carbon are actually taken 3 minutes later than they are plotted.

switching feeds, an air bubble developed in the line to the HPLC temporarily stalling the HPLC, causing the second drop in temperature.

It took several minutes for the JP-5 to flush the methanol from the line, but the delay was less than when water was changed to methanol, due to a higher flow. As the JP-5 entered the reactor, the temperature climbed again because of its higher heating value. We believe the large fluctuations in reactor temperatures occurred because the JP-5 is immiscible in water. Instead of feeding a uniform 7.5 wt% solution of JP-5 in water, we believe that short bursts of pure jet fuel were interspersed with bursts of pure water. Between 321 and 327 minute a mixture of JP-5 and methanol persisted, which resulted in smaller fluctuations. At 327 minutes, the magnitude and frequency of the temperature fluctuations increased as all the methanol was flushed out. Large, rapid fluctuations also occurred in the pressure and flow rate measurements. Despite the fluctuations, JP-5 was oxidized and reactor control was good.

At 345 minutes, air flow was discontinued; the temperature dropped, and TOC increased. At 358 minutes, NPA and EHM flow were changed to water and residual organic was flushed from the system.

3.4 TESTS WITH SALT: Subsequent to the methanol and JP-5 destruction tests, a test was done with a solution of sodium sulfate (Na_2SO_4) to study the salt deposition and transport behavior in the reactor with the injector. Many tests were done for the Army program to characterize the effectiveness of the platelet reactor in eliminating salt deposition and promoting salt transport through the reactor [10]. Although the platelet reactor was not completely successful at eliminating salt deposition, the deposition was restricted to the heating section at the top of the reactor. As discussed in Section 1, tests for the Army program used a reactor with radial injection of heating water. Hence, this test was done to investigate the effect of the injector on salt deposition or transport.⁵

For this test, the system was operated without air and without organic compounds in

the EHM and NPA inlet streams. The test conditions are shown in Table 6. The flow of water to the top platelet was increased to 3.8 gm/s (3.6 gallons per hour). EHM temperature was decreased to 230 °C (446 °F) and flow was increased to 0.9 gm/s (0.85 gallons per hour). At these conditions, the process temperature was 400 °C (752 °F). The EHM stream was switched to a 3 wt% salt solution by switching the inlet to the Milroyal pump. Figure 8 shows the conductivity data and the accumulated quantity of salt entering and leaving the reactor. Salt flowed for 25 minutes; a 5 minute initial pulse then a 20 minute sustained flow. Results were similar to previous salt tests with the radial injection. About 70 % of the salt came through the system. Changes in the effluent plumbing since the Army tests make the diagnostics less sensitive to spikes, but one large spike was evident, indicating that a large piece of salt broke loose from the wall and fell to the bottom of the reactor where it was dissolved in the subcritical water.

Two days after this test, the injector was removed for inspection and the reactor was opened. Salt was uniformly caked on the face of the injector about 6 mm (1/4 inch) thick as shown in Figures 9 and 10 (salt was also deposited on the thermocouples used to measure process temperature). A large chunk of salt, roughly 19 mm (3/4 inch) in diameter, was caught in the thermocouples below the injector as though it had fallen there. It was apparently not firmly attached to the injector and dislodged when the system was disassembled. Salt was deposited in a very thin layer on the reactor wall in the top 15 cm (6 inches). There was also a solid coating of salt on the top half of the bottom reactor section. We believe that the deposit in the bottom section is due to mal-distribution of the platelet water due to the low flow rate and low temperature on this test. If the platelet water is less than 373 °C (703 °F), it may act more like a dense liquid and not be distributed properly over the entire vertical surface of the reactor. That is, gravity has an affect. The differential pressure through the bottom platelet was only 2 bar (29 psi). This was significantly below the design condition of 13.8 bar (200 psi). It was run at this condition to reduce chiller demand or the amount of energy that must be removed from the effluent. We are currently at capacity. If chiller capacity is exceeded, control of the system is lost, necessitating reactor shut-down.

⁵ Salt deposition is not as much of a concern for the Navy EHM compounds as for the Army wastes although some Navy waste will contain salt.

We believe that the deposition in the injector region can be significantly reduced by introducing the injector face protection flow at temperatures less than 350 °C (662 °F). The solubility of sodium sulfate falls exponentially from 3 wt% at 350 °C (662 °F) to 0.04 wt% at 380 °C (716 °F) [14]. For the test described above, the temperature of the injector face protection flow was 450 °C (842 °F). The model presented at the end of this report predicts that 98.7% of the JP-5 would be destroyed in the EER at the conditions shown in Table 7. These conditions should minimize salt deposition, but funding and testing emphasis did not permit us to explore this possibility. JP-5 is less refractory than many chemicals that contain a high salt loading, nevertheless, these considerations are documented here, so that they may be explored at a later time.

3.5 TESTS TO DESTROY OIL: Chevron Delo 400 oil was destroyed in the EER in two separate tests. Procedures and conditions were similar to those used to destroy JP-5. Initial test conditions are shown in Table 8; test results are shown in Figure 11.

Process temperature at three inches below the face of the injector and TC, TIC, and TOC of the effluent, are shown in Figure 11. The NPA stream was switched from water to the NPA solution at 150 minutes. Due to TOC analyzer problems, the first accurate TOC sample was not collected until after 170 minutes. TOC measurement indicated only partial reaction of the NPA. The temperature and flow of the heating water were increased to 590 °C (1094 °F) and 2.6 gm/s (2.5 gallons per hour), respectively, and the injector face protection temperature was increased to 440 °C (824 °F), but the TOC decreased only slightly. At 190 minutes, the Milroyal pump supplying water to the EHM stream was turned-off leaving only the flow from the HPLC pump. The temperature climbed rapidly and TOC decreased as the NPA began to react. Due to concerns with chiller capacity, the temperature of the water to the lower platelet was reduced to 350 °C (662 °F).

At 200 minutes, the flow through the HPLC pump was switched to oil. As discussed previously, there is a long lag time before it reaches the reactor. To decrease this lag, the flow through the HPLC pump was increased at about 207 minutes resulting in an instantaneous increase in the flow of water into the reactor and a 20 °C (36 °F) dip in process temperature. Five minutes later, the HPLC flow rate was reduced;

then the Milroyal pump was restarted. A drop in process temperature of 50 °C (90 °F) ensued. After a delay of 5 more minutes, the oil reached the reactor and the process temperature increased by more than 200 °C (360 °F). TOC data show a negative value at 215 minutes. This is because the analyzer first measures TC, then IC about three minutes later and obtains TOC by subtraction. The TC sample was collected during the delay between Milroyal pump restart and the oil entering the reactor. During this delay, the temperature was low and NPA did not react completely, resulting in a TC reading of 150 ppm. The IC sample, however, was collected after the oil began to react and contained dissolved carbon dioxide from the reaction. The negative TOC value is an artifact of the different conditions when the two samples were taken. The level of IC in the effluent is a sensitive indicator of the total amount of organic that is reacted.

Although the NPA did not react to completion by itself, the NPA and oil together did.

Due to the rate of increase in process temperature, the flow rate of the oil from the HPLC was decreased. The temperature of the heating water and injector face protection water were also simultaneously decreased. At 230 minutes the flow rate was restored resulting in a process temperature of between 550 and 600 °C (1022 and 1112 °F). Large fluctuations in temperature may be due to the immiscibility of the oil in the water producing variations in the feed injection concentration as in the tests with JP-5.

At 234 minutes, the flow of water from the Milroyal was discontinued and undiluted oil was then injected into the reactor. The flow through the EHM line dropped immediately, but the concentration did not increase until the mixed fluid in the line was flushed out. Consequently, process temperature, IC, and TOC decreased due to an initial and immediate decrease in the amount of oil entering the reactor. Recall that the IC measurements are made about 3 minutes after the TOC measurements although they appear at the same plotted position. At 245 minutes, the undiluted oil entered the reactor. TC and IC returned to their previous levels (at the diluted conditions). However, process temperature climbed considerably higher, to 670 °C (1238 °F), because the water from the Milroyal pump no longer cooled the stream.

At 260 minutes, the flow of heating water was decreased to 2.1 gm/s (2 gallons per hour) resulting in a further increase in process temperature. The heating water was actually cooling the system because its temperature was less than the process temperature. At 263 minutes, the flow through the NPA circuit was switched from 15 wt% NPA to pure water. This is significant. At this point, the system was running without organic in the NPA circuit and with pure oil in the EHM circuit. Reactor temperature decreased to 530 °C (986 °F). TC and IC both decreased proportionately due to the decrease in organic input. Small fluctuations, which continued while pure oil and NPA were injected, disappeared when the NPA was discontinued.

At 270 minutes, the flow of water through the NPA circuit, which had drifted upwards to 0.8 gm/s (0.76 gallons per hour), was reduced to 0.3 gm/s (0.29 gallons per hour). This caused a small increase in the reactor temperature of about 15 °C (27 °F). At 285 minutes, the flow of oil was increased from 0.075 to 0.11 gm/s (0.07 to 0.10 gallons per hour). This caused a rapid increase in temperature to 670 °C (1238 °F). At 300 minutes, the temperature of the injector rinse water was reduced to 400 °C (752 °F) and the flow of heating water was reduced to 1.2 gm/s (1.14 gallons per hour), causing, at first, a decrease, and then, an increase in reactor temperature. Operating conditions at the end of the test are given in Table 9.

Temperatures at one and five inches were both less than at the three inch location, shown in the figure, indicating a primary reaction zone at three inches. DRE was 0.985 +/- 0.005.

This test was repeated as test 11. We intended to execute a destruction test at stable or unchanging conditions with flows and temperatures at the nominal design conditions. The system was brought to temperature with water flowing through both the EHM and NPA circuits with the air off. Flow to the EHM circuit was again provided by two pumps, a Milroyal and an HPLC pump. Difficulty in priming the Milroyal pump was experienced; this pump's setting was increased above normal to establish flow. Test conditions at 90 minutes are shown in Table 10. Process temperatures at one, three, six, and ten inches below the injector face are plotted in Figure 12.

At the conditions shown in Table 10, the process temperature was 390 °C (734 °F). Air

flow was initiated at 95 minutes resulting in a sudden drop in temperature to 350 °C (662 °F). Previous tests had established that the NPA will not react with air if water is flowing through the EHM circuit. The flow through the EHM circuit was discontinued at 97 minutes prior to the introduction of NPA at 100 minutes.⁶

At 100 minutes, the flow through the NPA circuit was switched from water to a 15 wt% solution of NPA. Simultaneously, the flow through the HPLC pump was switched to 100 % oil. Within a few seconds, the NPA solution was injected into the reactor, but the oil, with a much lower flow rate and longer supply line, did not reach the injector port until 12 minutes later. Initially, the temperature in the reactor remained constant and the TOC increased to greater than 200 ppm indicating that the NPA did not react. However, as the oil reached the reactor, the temperature jumped abruptly from 390 °C to 700 °C (734 to 1292 °F). The TOC stabilized at 60 to 70 ppm. This is higher than the 50 ppm plateau obtained on the previous test. It may be a result of the lower wall protection water temperature used for this test.

After 50 minutes of injecting the oil, the differential pressure across the injector on the EHM circuit began to increase. Several unsuccessful attempts were made to reduce the differential pressure by diluting the oil with water at the injection port. At 164 minutes the oil was switched to pure water at the HPLC pump and the flowrate was increased to try to flush the line in preparation for termination of the test. At 180 minutes, the EHM circuit differential pressure increased to 300 psi. At 195 minutes the test was terminated.

On the next workday, the injector was "back-flushed." Although 4.1 bar (60 psi) backpressure was needed to develop any flow, no significant differential pressure was measured across the injector. This indicated a blockage upstream of the injector (downstream during the backflush). At 4.1 bar (60 psi) reactor pressure, a small backflow started through the EHM line consisting of a thick, oily sludge. This line was flushed for 1/2 hour.

⁶ The Milroyal pump remains on but the stream is diverted into an overflow tank. Pure water is injected into the reactor during start-up, in this manner, to gradually heat all components to high temperature. This technique minimizes the chance for "leaks" due to thermal expansion.

Filters on this line were removed and found to be caked with thick residue that filled the entire filter housing. These filters were not inspected between tests; we do not know if this residue is the result of a cumulative process or the result of this single test. It was brownish, like the oil, and had a strong odor. Consistency varied from a thick axle grease to a hard, solid wax. Flakes of the wax-like material as thick as 1.5 mm (1/16 inch) had broken loose in places, but, in general, the residue was extremely difficult to remove. With the filters removed, little pressure drop occurred across the injector and the water flowed clear.

We infer, from this data, that we either formed or separated from the oil, a thick, foul smelling compound that plugged the filters.

3.6 TEST TO DESTROY HYDRAULIC FLUID: Finally, Velsicol H-537 hydraulic fluid was destroyed at temperatures in excess of 620 °C (1148 °F). Reactor test conditions are shown in Table 11. The EHM stream was not preheated for this test.

Process temperature at 1, 3, 5, and 10 inches are shown in Figure 13. The system was heated to process temperature with pure water in the EHM stream. At $t = 0$ minutes, air was injected into the reactor, dropping the temperature by 50 °C (90 °F). Simultaneously with injecting the air into the reactor, the EHM stream was switched to hydraulic fluid. This is a different sequence for EHM destruction than the previous tests. Little reaction occurred.

NPA was injected at $t \sim 35$ minutes resulting in initiation of the reaction and a prompt increase in process temperature of 620 °C (1148 °F) (the reason for the slight decrease in temperature at $t \sim 20$ minutes is a temporary increase in flowrate of one of the pumps). Peak temperature occurred three inches from the face of the injector.

The differential pressure across the EHM orifice is also plotted on Figure 13. During the test it increased continually from a base of 1.4 bar (20 psi), rising sharply at $t = 45$ minutes to 34.5 bar (500 psi). The test was terminated to prevent damage to the injector. TOC measurements were unstable throughout the test, precluding DRE determination. The reason for injector pluggage is unknown. Small specs or deposits of a brown, powdery substance were observed on the face of the injector and the top 10 mm (0.4 inch) of the reactor when it was opened after the test.

3.7 IMPLICATIONS FOR FULL SCALE SYSTEM: The test results compared favorably with theory, and to the DREs and the rate constant work generated in the first phase of this program. This confirms that the transpiring wall reactor does not adversely affect the destruction chemistry.

The tests demonstrated that the injector works as intended; the NPA initiated the reaction of the EHM to CO₂. More significantly, once the reaction of the EHM was initiated, it was self sustaining without the NPA. Both the NPA and the EHM were needed initially since neither stream reacted by itself at nominal flow rates and temperatures.

Large temperature fluctuations occurred when the EHM was not miscible in water. This did not have an obvious effect on system performance, but may be a factor if JP-5 is used as the auxiliary fuel instead of NPA.

The only significant problem was the plugging in the inlet lines and the injector that occurred with both the oil and the hydraulic fluid. Although the exact cause was not determined, it may be necessary to inject the fluids at room temperature to prevent formation of viscous compounds. Also, the orifices in the injector should be as large as possible.

MODEL

4.1 INTRODUCTION: Program Inj is a code developed to predict the temperature profile in the EER with the transpiration wall reactor and multi-stream injector. A heat release model is encoded for the three compounds, JP-5 jet fuel, H-537 hydraulic fluid, and Delo 400 Chevron oil. In addition, temperature profiles can be generated for methanol as the simulated EHM.

NPA is the fuel used for the chemical spark plug in the center of the injector. The injector has five streams entering at different temperatures: 1) the hot water stream, used to bring the air and fuel to high temperature, entering at \dot{m}_h gm/s and T_h , 2) the injector face protection stream, used to protect the face of the injector from corrosion and salt deposition, entering at \dot{m}_d gm/s and T_d , 3) the fuel stream, used to initiate the reaction, entering at \dot{m}_{NPA} gm/s and T_{NPA} , 4) the air stream, used to convert the EHM to CO₂, entering at \dot{m}_a gm/s and T_a , and 5) the EHM stream that is being converted, entering at \dot{m}_w gm/s and T_w .

4.2 GRAPHICAL USER INTERFACE (GUI): Figure 14 shows the GUI. The code has been developed in Visual BASIC 4.0 in the Windows 95 32 bit environment. At the top left are four user buttons. The "Calculate" button generates a temperature profile, the "Print" button prints results, the "Clear" button clears the values in the input boxes, and the "End" button ends all calculations.

In addition to the streams that enter the injector, two other streams enter the reactor portion at flow rates \dot{m}_{p1} and \dot{m}_{p2} gm/s at temperatures T_{p1} and T_{p2} , respectively. \dot{m}_{p1} is the flow rate associated with the top portion of the reactor (the top 18 inches) and \dot{m}_{p2} is the flow rate associated with the bottom portion of the reactor (the second 18 inches). It is these streams that constrain the organic stream to a central core region.

x is the total reactor length which should always be input as 36 inches. This assumption is currently hard-coded. w is the weight percent as a decimal fraction for the NPA and ww is the weight percent for the EHM, also as a decimal fraction. f and fw are returned by the code and are, respectively, the fraction of NPA and EHM that are converted.

In the lower left panel is the EHM that must be selected before pressing the "Calculate" button. In the central listbox, the reactor position, temperature, and integrated residence time (returned by the code) are printed. Temperature as a function of position is graphed in the lower right. The final box is a place for notes to be written before printing the results.

The user inputs all parameters other than f and fw , selects a EHM and then presses "Calculate".

4.3 MODEL DEVELOPMENT: A copy of the code is provided in Appendix A. It is divided into several subroutines that are coded in a procedural and structurally oriented manner. The main routine is located in Private Sub cmdCalc_click (). cmdCalc is the "object" button located on the GUI that is the "Calculate" button. The event is "click" and is actuated when the user presses this button. This main routine calls several subroutines in the following order (all parameters are passed by reference):

1) readin reads the user input from the GUI,

2) enthalpy passes as parameters enthalpy and temperature. enthalpy calculates the enthalpy of water by using temperature and the steam tables at 240 bar (3480 psi). h_a is the enthalpy of the air which is calculated using an assumed constant specific heat. The enthalpy input at each location is calculated in this fashion and assigned to the variable h_{lsh} .

3) eq_temp_at_x is then called to find the local thermodynamically assumed equilibrium temperature at x .

4) res_time_at_x is then called to find the residence time from x to $x+1$.

5) heat_release_at_x is finally called to find the heat released.

The results are then graphed and printed to the GUI. The modeling in terms of these subroutines is discussed in the next sections.

Enthalpy:

By conservation of energy, the enthalpy at location x is equal to

$$\dot{m}_h h_h + \dot{m}_{NPA} (h_{NPA} + f\lambda) + x \dot{m}_p h_p + \dot{m}_d h_d + \dot{m}_w h_w + \dot{m}_a c_p T_a = h_{lsh}. \quad (1)$$

After making this assignment, the eq_temp_at_x function is called and temperature is iterated on until $h_{lsh} = h_{rsh}$, that is, until a uniform homogeneous temperature is reached. h is monotonically increasing and this fact is used during the iterative procedure. Several assumptions are inherent in Equation (1), primarily the assumptions of local thermodynamic equilibrium and one-dimensionality.

Residence time:

To calculate residence time it is necessary to assume a flow model. The model used is the homogeneous flow model which states that the velocity of air, V_a , is equal to the velocity of the water, V_w ,

$$V_a = V_w = V. \quad (2)$$

This is probably an appropriate assumption in the absence of detailed experimental data on flow regimes at supercritical conditions. With this assumption the total flow rate, \dot{m}_T is given by

$$\dot{m}_T = \rho_a(AV)_a + \rho_w(AV)_w = \rho(AV). \quad (3)$$

Defining

$$A = A_a + A_w, \quad (4)$$

equations (2), (3), and (4) are combined to yield

$$\rho = (A_a/A) \rho_a + (A_w/A) \rho_w. \quad (5)$$

By defining

$$A_a/A = \alpha, \quad (6)$$

equation (5) becomes

$$\rho = \alpha \rho_a + (1 - \alpha) \rho_w. \quad (7)$$

In 2- ϕ flow models, α , is formally known as the void fraction. We retain this terminology while recognizing that the term "void fraction" is not applicable at these conditions. α is calculated by observing that

$$\begin{aligned} \alpha &= A_a / (A_a + A_w) \\ &= (\dot{m}_a / \rho_a) / (\dot{m}_a / \rho_a + \dot{m}_w / \rho_w). \end{aligned} \quad (8)$$

To summarize to this point, the energy equation, equation (1), is used to first find the local thermodynamic temperature, T_{eq} . ρ_a and ρ_w are then calculated from equations of state for ideal mixtures. The `res_time_at_x` subroutine is then called to determine V , given the above equations and assumptions. The residence time, dt , at temperature T_{eq} is then computed from

$$dt = dx / V. \quad (9)$$

An additional assumption inherent in the above model, is the assumption of ideal mixtures. We have not verified this assumption and an improved model may lead to changes in the calculated values of residence time.

Heat Release:

Rate constants based on TOC analysis were generated in Phase I of our work. A one-step heat release model is developed and coded as part of this work as follows: The rate of change in the concentration of any organic N is proportional to the concentration, where the proportionality constant is defined as the rate constant,

$$-d[N]/dt = K[N] \quad (10)$$

Integrating (10) yields

$$[N] = [N_0] e^{(-Kt)} \quad (11)$$

where $[N_0]$ is the initial concentration.

The fraction, f , converted over a distance dx , is found by noting that

$$([N_0] - [N])/[N_0] = 1 - e^{(-Kt)} \quad (12)$$

If $[N_0]$ is the concentration at $x = 0$, $[N_1]$ is the concentration at $x = 1$, and $[N_j]$ is the concentration at $x = j$, then

$$\begin{aligned} f &= f_1 + f_2 + \dots + f_j + \dots + f_n \\ &= 1 - [(1-f_1)(1-f_2)\dots(1-f_j)\dots(1-f_n)] \end{aligned} \quad (13)$$

These equations are coded in `heat_release_at_x` and `heat_releasew_at_x` subroutines and called after `res_time_at_x`.

There is a subtle modeling assumption inherent in the above equation: We assume that the heat release is a one-step and prompt process; a molecule of EHM or fuel is converted to CO_2 with no time delay.

4.4 COMPARISON WITH DATA: In Figures 15, 16, and 17, data are generated for the destruction of JP-5, Oil, and the Hydraulic fluid, respectively. The mixing temperature of all the fluids that enter the injector is predicted at $x = 0$. Temperatures increase from this base value as heat is released by NPA and the EHM. Peaks that vary as to amplitude are predicted between $x = 0$ to $x = 12$ inches.

In general, the location of the peak temperature in the model is several inches below the location observed experimentally. Recall that, internally within the injector, the single inlet stream of air is split into two streams, one that mixes with the hot water injection stream, and the second that mixes with the EHM. The air, hot water injection stream, and NPA, then react to increase temperature locally. This energy is then transported to the bulk to initiate the conversion of EHM to carbon dioxide. If working properly, we expect the reaction zone to be concentrated towards the top of the injector.

This phenomena is not modeled in the work presented above, and indeed, is a nearly impossible problem to model. The fact that the experimentally observed reaction zone occurs at locations before what this model predicts is consistent with this line of reasoning.

The model predicts 1 % greater DRE than observed experimentally. This may necessitate an increase in reactor design length. The phenomena that is causing this has not been identified. It may be due to a layer of cooler fluid adjacent to the transpiration boundary layer where reaction rates are retarded in comparison to the core flow but this is purely speculative.

SUMMARY AND CONCLUSIONS

Tests described in this report concentrated on destroying specific Navy EHM streams to demonstrate the viability of a transpiration wall reactor to destroy Navy excess hazardous materials (EHM). The transpiration wall reactor is a novel chemical reactor developed by Gencorp Aerojet corporation that is intended to constrain the reacting organic to a central core region. By preventing contact of reacting species with the walls, it inhibits deposition of sticky salts and reduces corrosion of reactor wall material.

A multistream injector is an integral part of the overall reactor concept. Air, a fuel such as NPA, hot water to initiate a reaction with the NPA, injector protection water, and an EHM are all injected into the reactor through the multistream injector. Tests concentrated on initiating the destruction of the EHMs by using the injector and in proving out the injector concept.

Jet fuel, JP-5, was destroyed at process temperatures in excess of 650 °C (1202 °F) to 98.5 % in less than 4.8 seconds. Oil was also destroyed to 98.5 % in less than 4.8 seconds. Due to experimental problems we could not determine the DRE of the hydraulic fluid, but destruction phenomena were similar to the other two compounds. The model presented in the report, and the investigations in [13], indicate it should be similar to that of the JP-5. These results are consistent with basic chemical reaction data generated and documented in reference [13] as part of the Navy contract.

An engineering model was developed that predicts the key performance variables of temperature and destruction rate efficiency of the

Navy EHM in the Engineering Evaluation Reactor. The injector is designed to first mix the air, NPA fuel, and heating water. The NPA then releases energy and instigates the conversion of EHM to carbon dioxide. This is a more complicated situation than modeled here. However, this three-stream temperature can be calculated using the above code. The mixing of the resultant streams with the bulk fluid (the other streams) is a more complicated phenomena than can not be modeled.

The above model does predict residence time, which cannot be directly measured, a one-dimensional axial temperature profile at every location in the reactor, which also cannot be directly measured, and DRE which was compared to experiment.

The injector tests were successful. NPA initiated the reaction of the EHM to CO₂ and the EHMs were successfully destroyed. The results compared favorably with theory, and to the DREs and the rate constant work generated in the first phase of this program.

REFERENCES

1. S. F. Rice, R. R. Steeper, and C. A. LaJeunesse, "Destruction of Representative Navy Wastes Using SCWO," SAND94-8203, 1993.
2. S. F. Rice, C. A. LaJeunesse, et. al., "Efficiency of Supercritical Water Oxidation for the Destruction of Industrial Solvent Waste," 5th Symposium on Emerging Technologies in Hazardous Waste Management, Sept., 1993.
3. "Supercritical Water Oxidation of Colored Smoke, Dye, and Pyrotechnic Compounds", WFO proposal 83920103, ARDEC / DOE - Sandia.
4. C. A. LaJeunesse, et. al., "SCWO of Colored Smoke, Dye, and Pyrotechnic Compositions Final Report: Pilot Plant Conceptual Design," SAND94-8202, 1993.
5. S. F. Rice, C. A. LaJeunesse, et. al., "Supercritical Water Oxidation of Colored Smoke, Dye, and Pyrotechnic Compositions (Phase One Final Report)," SAND94-8209, 1994.
6. C. A. LaJeunesse, et. al., "Salt Deposition Studies in a Supercritical Water Oxidation Reactor (Interim Report)," SAND94-8201, 1993.

7. C. A. LaJeunesse and S. F. Rice, "Corrosion and Salt Deposition Issues in a Supercritical Water Oxidation Reactor," First International Conference on Advanced Oxidation Technologies for Water and Air Remediation, London, Ontario, Canada, June, 1994.
8. J. P. Chan, C. A. LaJeunesse, et. al., "Experimental Techniques to Determine Salt Formation and Deposition in Supercritical Water Oxidation Reactors," ASME conference, Chicago, Ill., Nov., 1994.
9. B. L. Haroldsen, et. al., "Transpiring Wall Supercritical Water Oxidation Test Reactor Design Report," SAND96-8213, 1996.
10. B. L. Haroldsen, et. al., "Transpiring Wall Supercritical Water Oxidation Reactor Salt Deposition Studies," SAND96-8255, 1996.
11. H. H. Mueggenburg, et. al., "Platelet Actively Cooled Thermal Management Devices," 28th Joint AIAA/SAE/ASME/ASEE Propulsion Conference, Nashville, TN, July, 1992.
12. C. A. LaJeunesse, et. al., "Supercritical Water Oxidation of Ammonium Picrate," SAND95-8202, 1994.
13. S. F. Rice, et. al., "Kinetic Investigation of the Oxidation of Naval Excess Hazardous Materials in Supercritical Water for the Design of a Transpiration-Wall Reactor, SANDxx-xxxx, 1996 (In progress).
14. D. Rousar, et. al., "Development of Components for Waste Management Systems Using Aerospace Technology," 46th International Aeronautical Congress at Oslo, Norway, Oct 2-6, 1995, Published by The American Institute of Aeronautics and Astronautics.
15. "U.S. Patent No. 5,387,398", Feb. 7, 1995, "Supercritical Water Oxidation Transpiration Reactor." Aerojet - General Corp.
16. F. J. Armellini and J. W. Tester, "Experimental Methods for Studying Salt Nucleation and Growth from Supercritical Water," Journal of Supercritical Fluids, Vol 4, No 4, 1991.

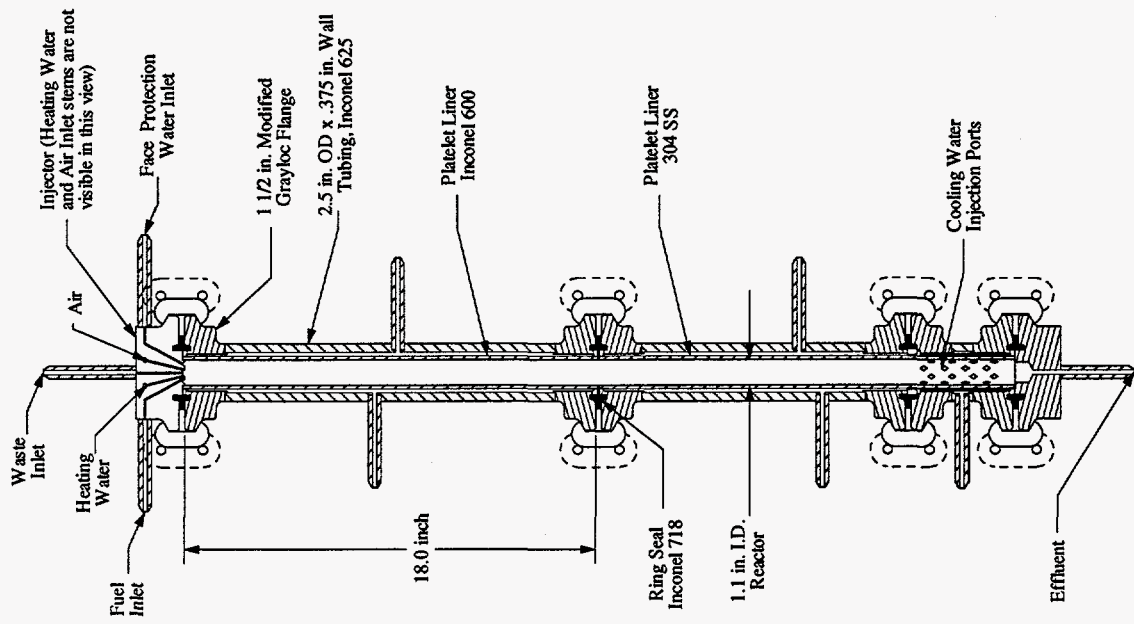


Figure 2. The test reactor is a 1/4 scale version of the prototype.

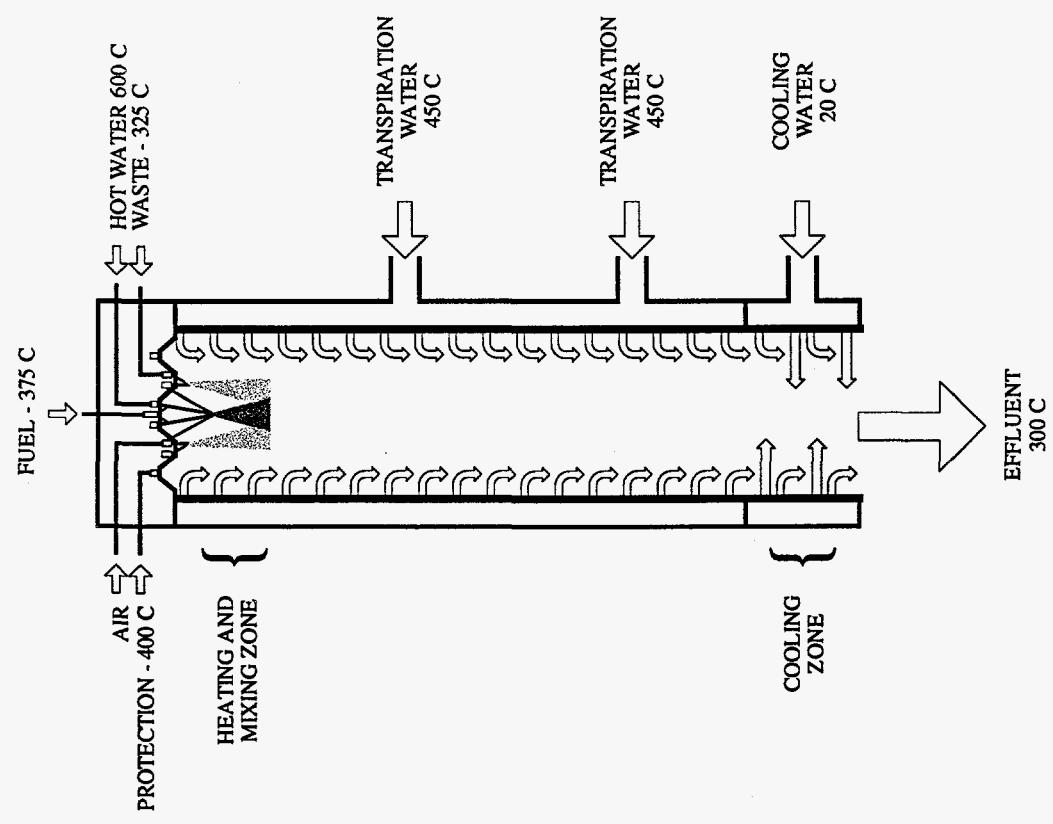


Figure 1. Conceptual operation of the transpiring wall reactor showing the various fluid streams.

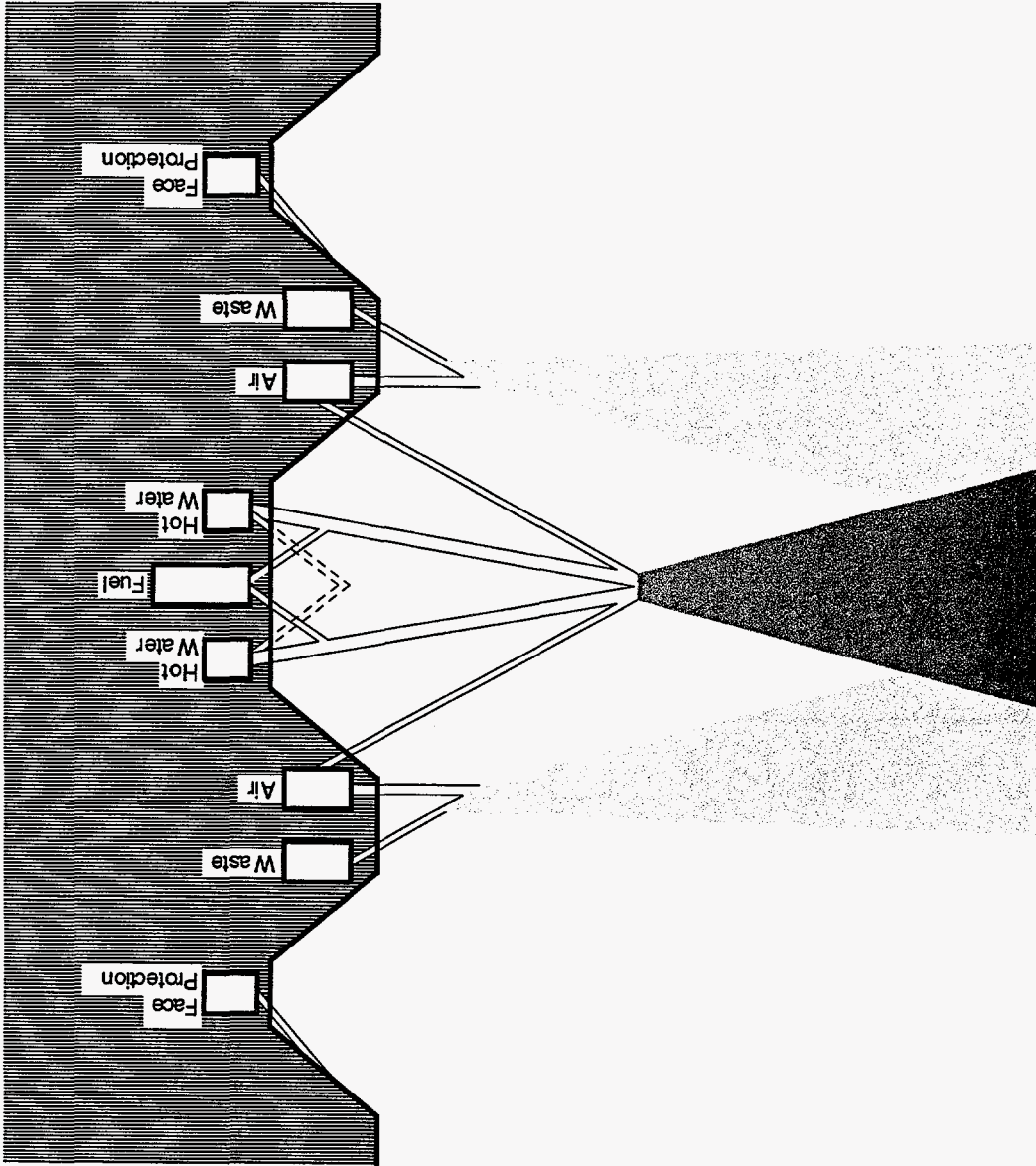


Figure 3. Cross-sectional illustration of the streams entering the reactor region from the injector.

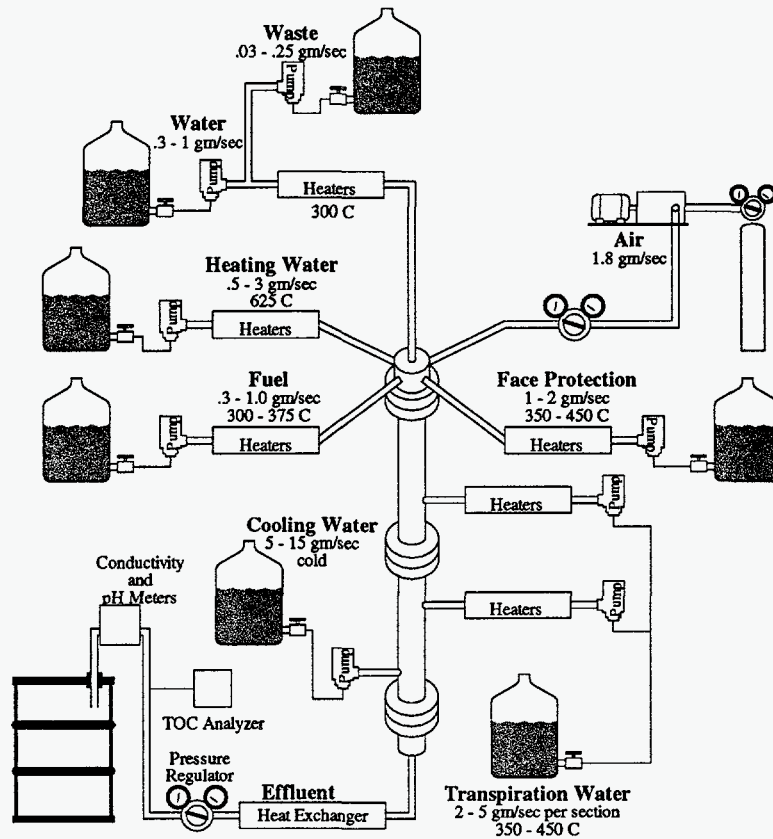


Figure 4a. Schematic of Sandia's Engineering Evaluation Reactor (EER) configured to test the transpiring wall reactor.

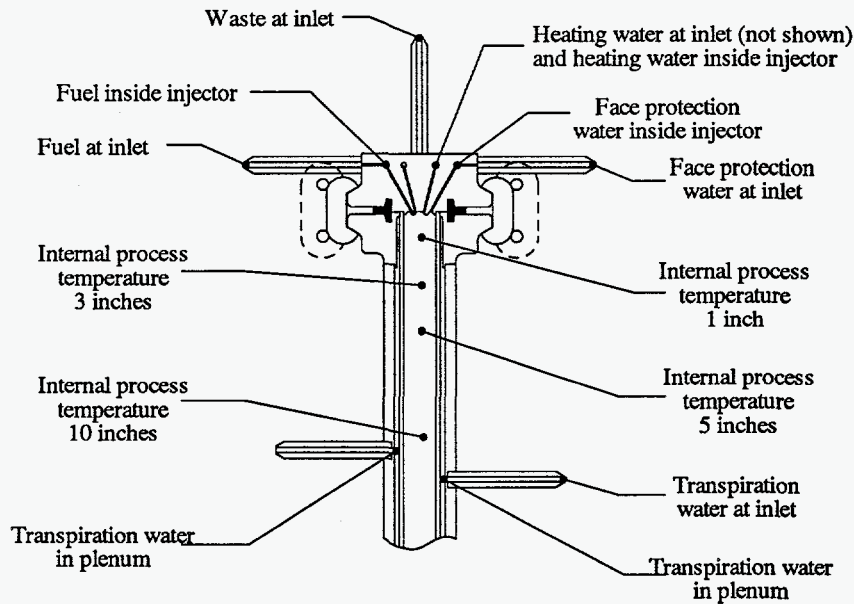


Figure 4b. Schematic showing the location of thermocouples in the top reactor section to measure fluid temperatures. Thermocouples were located in similar locations in the bottom section. Absolute and differential pressure measurements were made through the same instrumentation ports.

Table 1. Test Summary.

ID	Intent	EHM	Result
1	Trouble shoot system	N/A	N/A
2	Test injector w/NPA	N/A	Controller failed
3	Test injector w/NPA	N/A	No reaction
4	Test injector w/NPA	N/A	Plugged injector
5	Test injector w/NPA	N/A	Bad flowmeter
6	Test injector w/NPA	N/A	NPA reacted
7	Test injector w/NPA	N/A	NPA reacted
8	Destroy EHM	Methanol/JP-5	Materials destroyed
9	Test injector w/salt	N/A	Deposition
10	Destroy EHM	oil	Materials destroyed
11	Destroy EHM	oil	Materials destroyed
12	Destroy EHM	hydraulic fluid	Materials destroyed

Table 2. Test conditions for sixth test (NPA initiation).

Stream	Flow rate (gm/s)	Temperature (C)
EHM	0.5	390
NPA	0.3	390
Face protection	0.75	590
Heating water	2 - 3	590
Top platelet	3	460 - 600
Bottom platelet	3	460 - 600

Table 3. Design conditions.

Stream	Flow rate (gm/s)	Temperature (C)
EHM	1.0	325
NPA	0.45	375
Face protection	1.1	400
Heating water	1.1	600
Top platelet	5.0	subcritical
Bottom platelet	5.0	subcritical

Table 4. Test conditions for seventh test at 295 minutes (NPA initiation).

Stream	Flow rate (gm/s)	Temperature (C)
EHM	0.58	260
NPA	0.65	380
Face protection	off	N/A
Heating water	1.9	580
Top platelet	2.9	440
Bottom platelet	3.6	380

Table 5. Test conditions for eighth test (methanol and JP-5).

Stream	Flow rate (gm/s)	Temperature (C)
EHM	1.1	300
NPA	0.6	380
Face protection	1.0	450
Heating water	1.75	575 - 670
Top platelet	2.2	410 - 460
Bottom platelet	1.7	370 - 380

Table 6. Test conditions for ninth test (tests with salt).

Stream	Flow rate (gm/s)	Temperature (C)
EHM	0.9	230
NPA	N/A	N/A
Face protection	1.0	450
Heating water	1.75	560
Top platelet	2.2	410 - 460
Bottom platelet	1.7	370 - 380

Table 7. Input conditions to model.

Stream	Flow rate (gm/s)	Temperature (C)
EHM	1.1	300
NPA	0.1	400
Face protection	1.1	340
Heating water	1.9	620
Top platelet	5	450
Bottom platelet	5	450

Table 8. Initial test conditions for tenth test (tests with oil).

Stream	Flow rate (gm/s)	Temperature (C)
EHM	0.53	275
NPA	0.65	375
Face protection	1.2	400
Heating water	1.5	560
Top platelet	4.76	400
Bottom platelet	4.60	400

Table 9. Operating conditions at the end of the tenth test (tests with oil).

Stream	Flow rate (gm/s)	Temperature (C)
EHM	0.11	160
NPA	0.3	375
Face protection	1.2	400
Heating water	1.2	550
Top platelet	4.76	390
Bottom platelet	4.60	360

Table 10. Test conditions at 90 minutes for the eleventh test (test with oil).

Stream	Flow rate (gm/s)	Temperature (C)
EHM	1.1	300
NPA	0.6	380
Face protection	1.0	450
Heating water	1.75	575 - 670
Top platelet	2.2	410 - 460
Bottom platelet	1.7	370 - 380

Table 11. Test conditions for test 12 (test with hydraulic fluid).

Stream	Flow rate (gm/s)	Temperature (C)
EHM	0.06	30
NPA	0.6	380
Face protection	1.35	470
Heating water	1.13	580
Top platelet	7.0	380
Bottom platelet	5.5	325

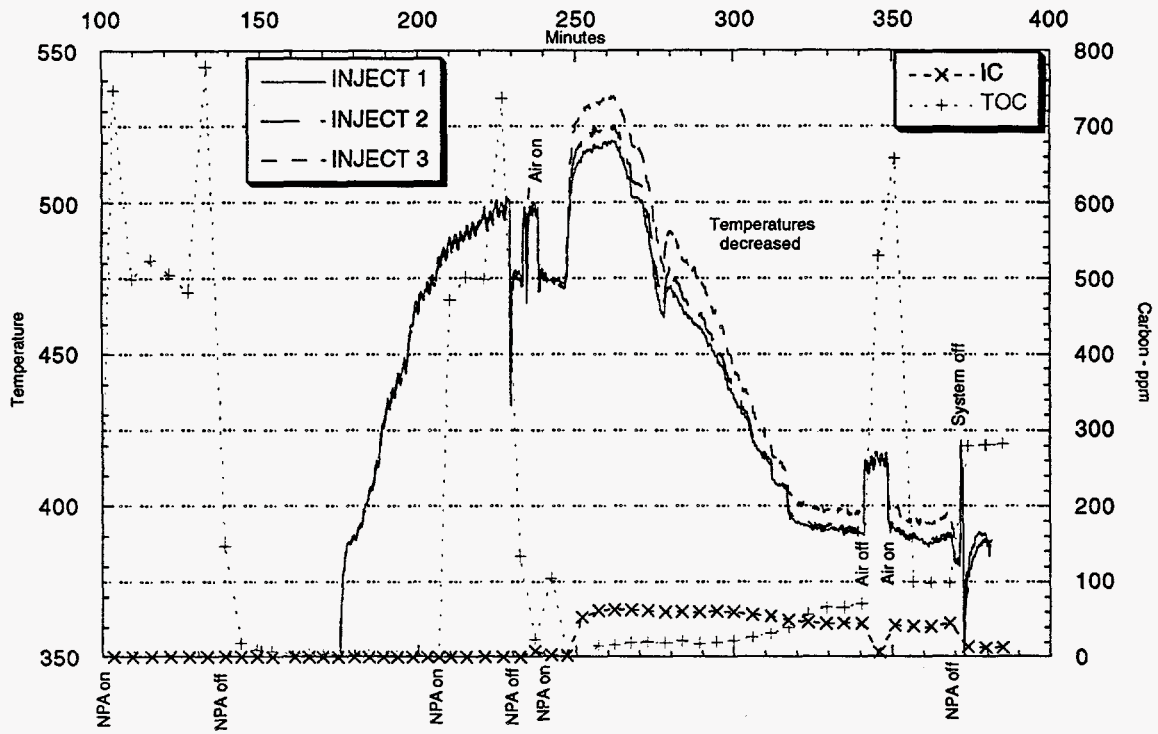


Figure 5. Process temperature, TC, TIC, and TOC (sixth test - NPA initiation).

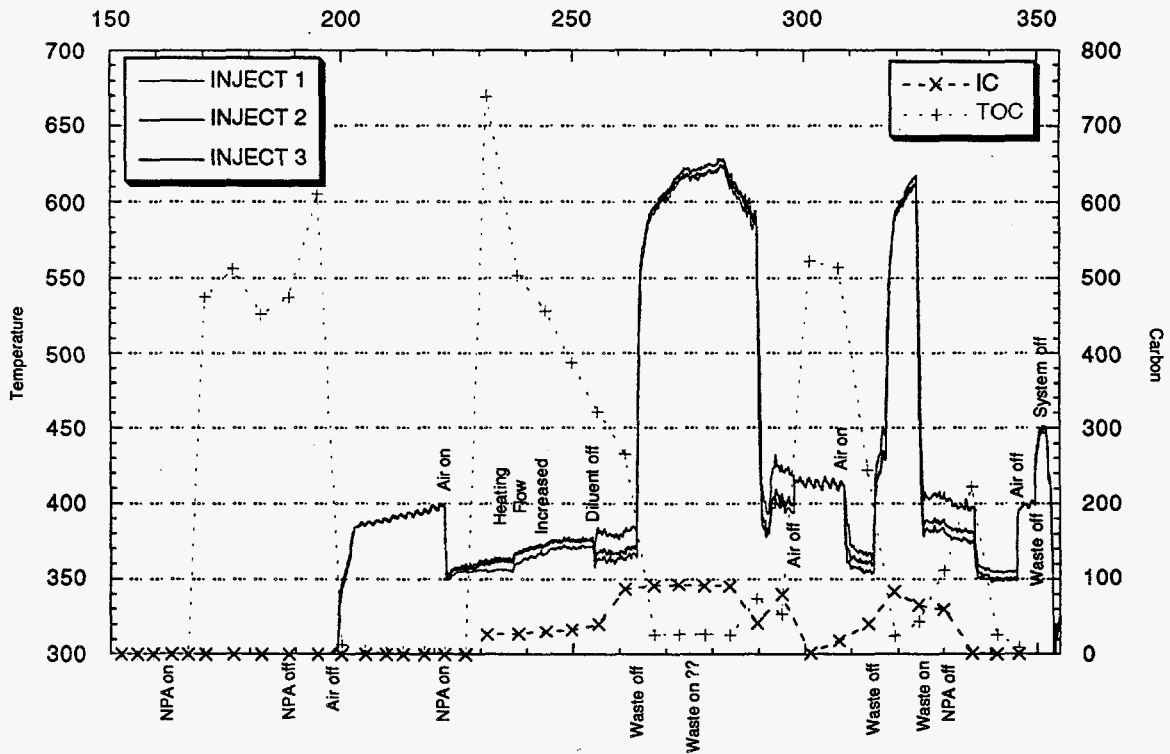


Figure 6. Process temperature, TC, TIC, and TOC (seventh test - NPA initiation).

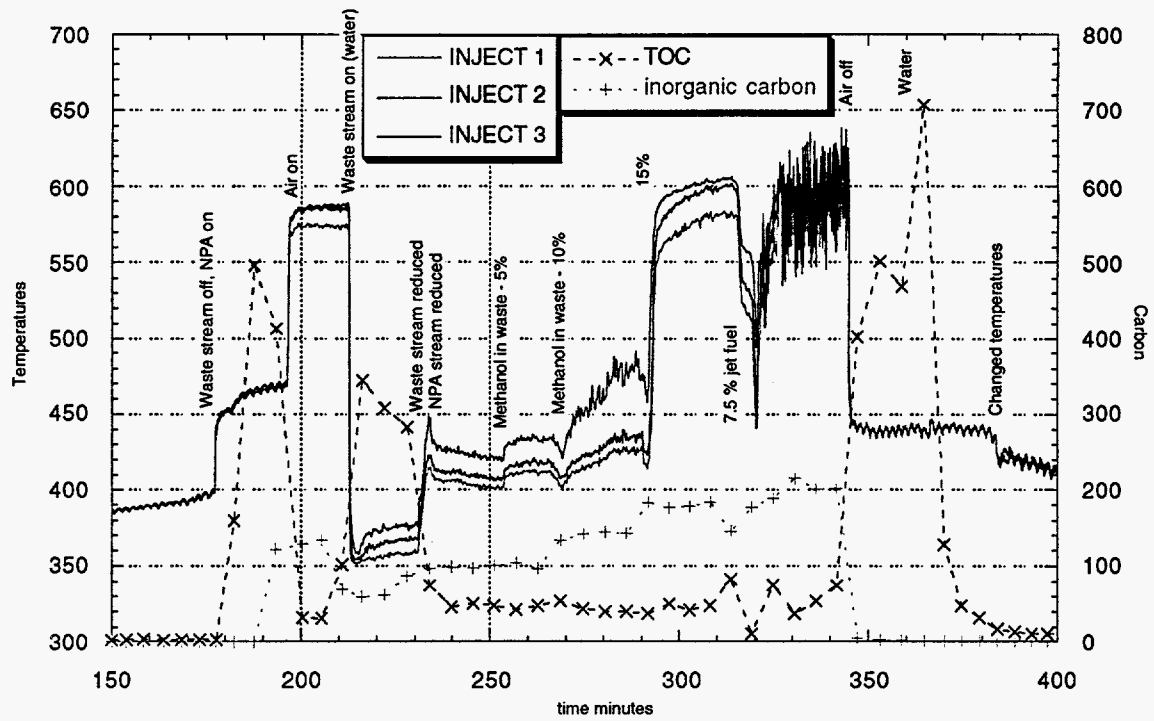


Figure 7. Process temperature, TC, TIC, and TOC (eighth test - Methanol/JP-5).

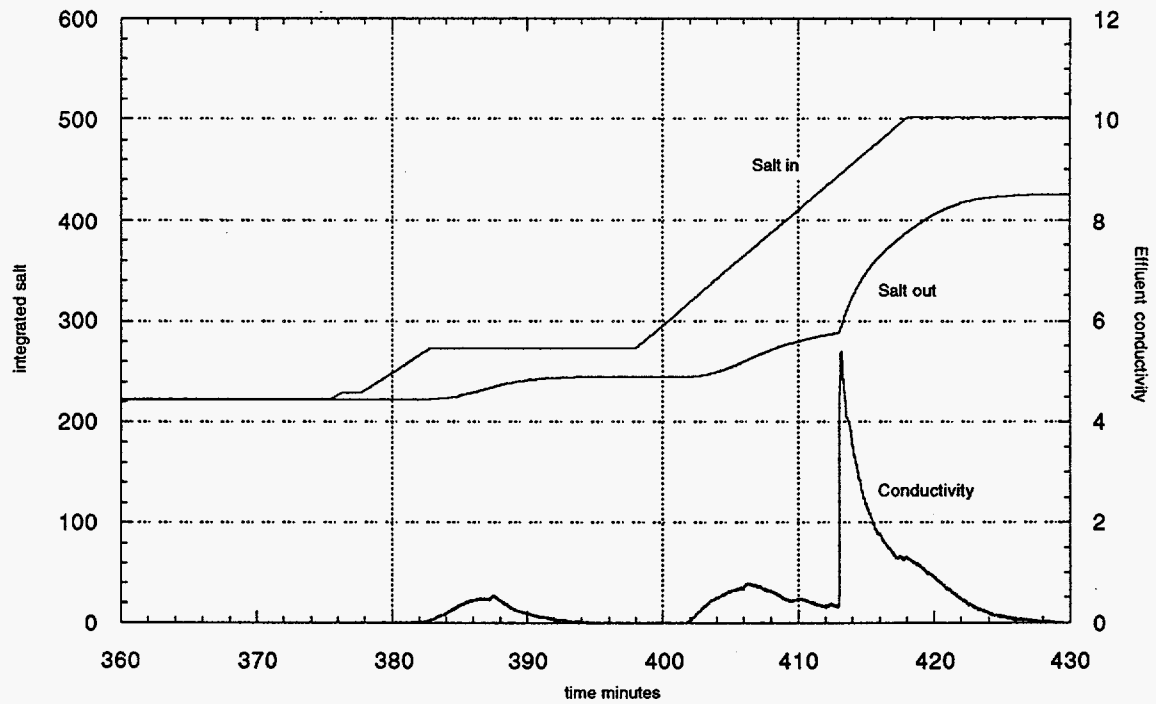


Figure 8. Conductivity data/salt balance (ninth test).

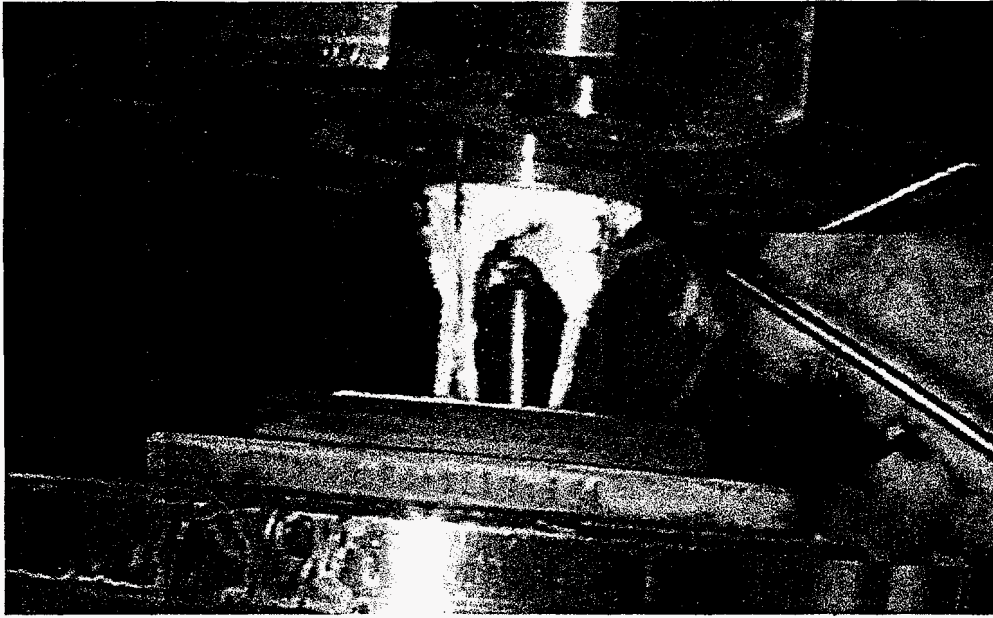


Figure 9. Salt Deposition photo (ninth test).



Figure 10. Salt Deposition photo (ninth test).

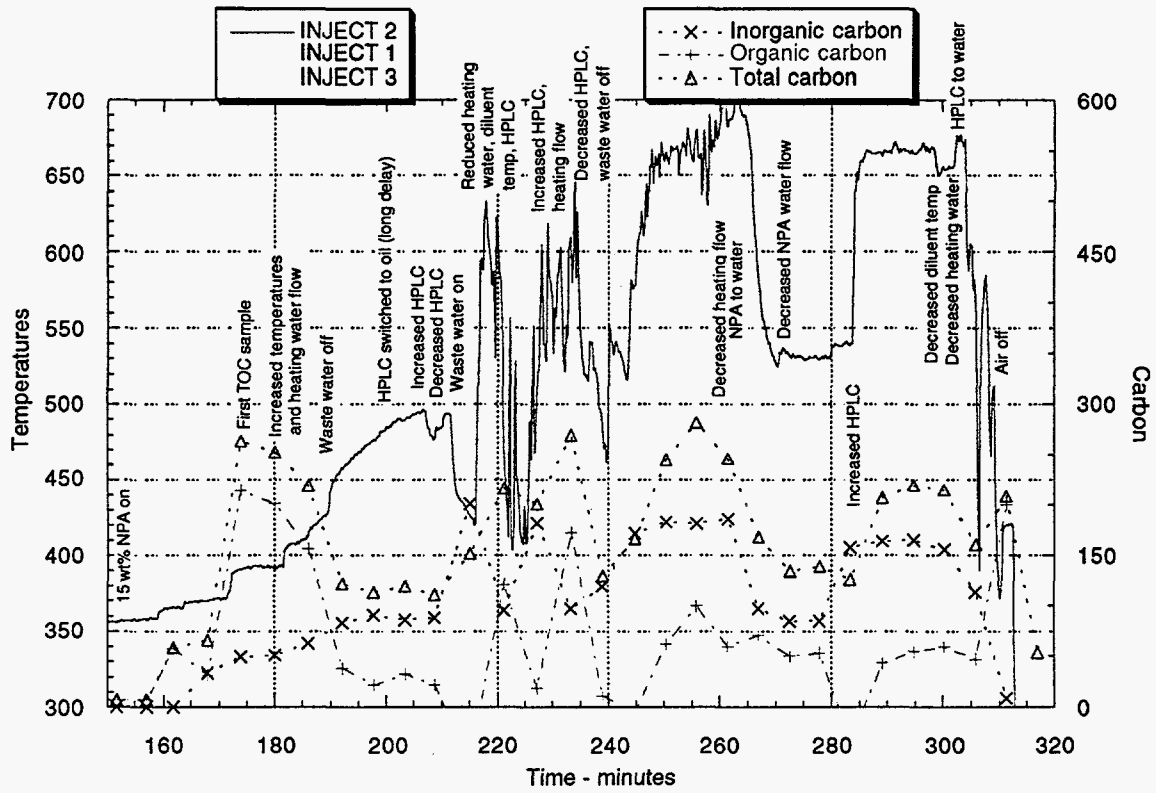


Figure 11. Process temperature, TC, TIC, and TOC (tenth test - Oil).

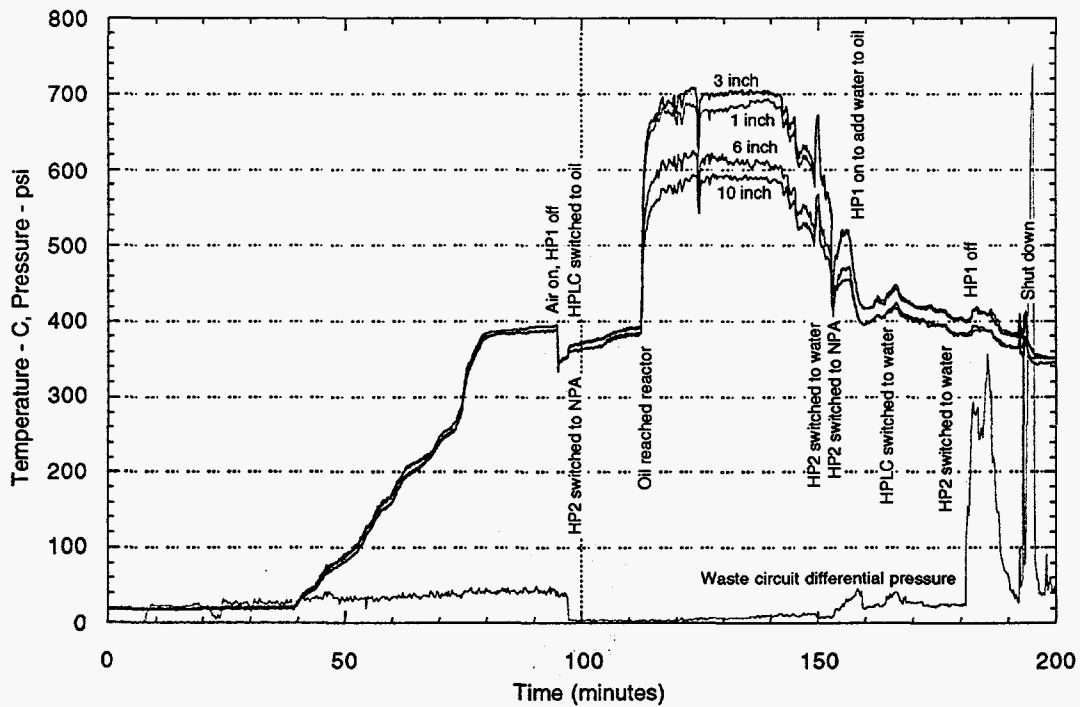


Figure 12. Process temperature and differential pressure (eleventh test - Oil).

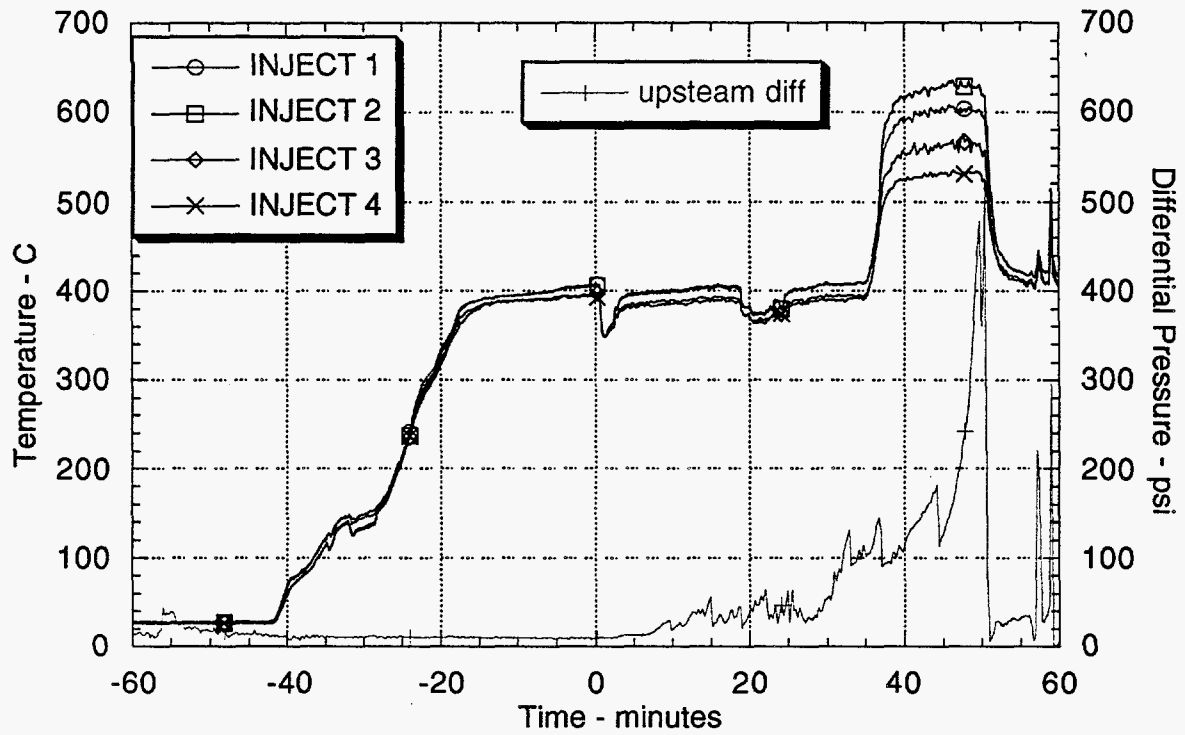


Figure 13. Process temperature and EHM orifice pressure differential (twelfth test - Hydraulic Fluid).

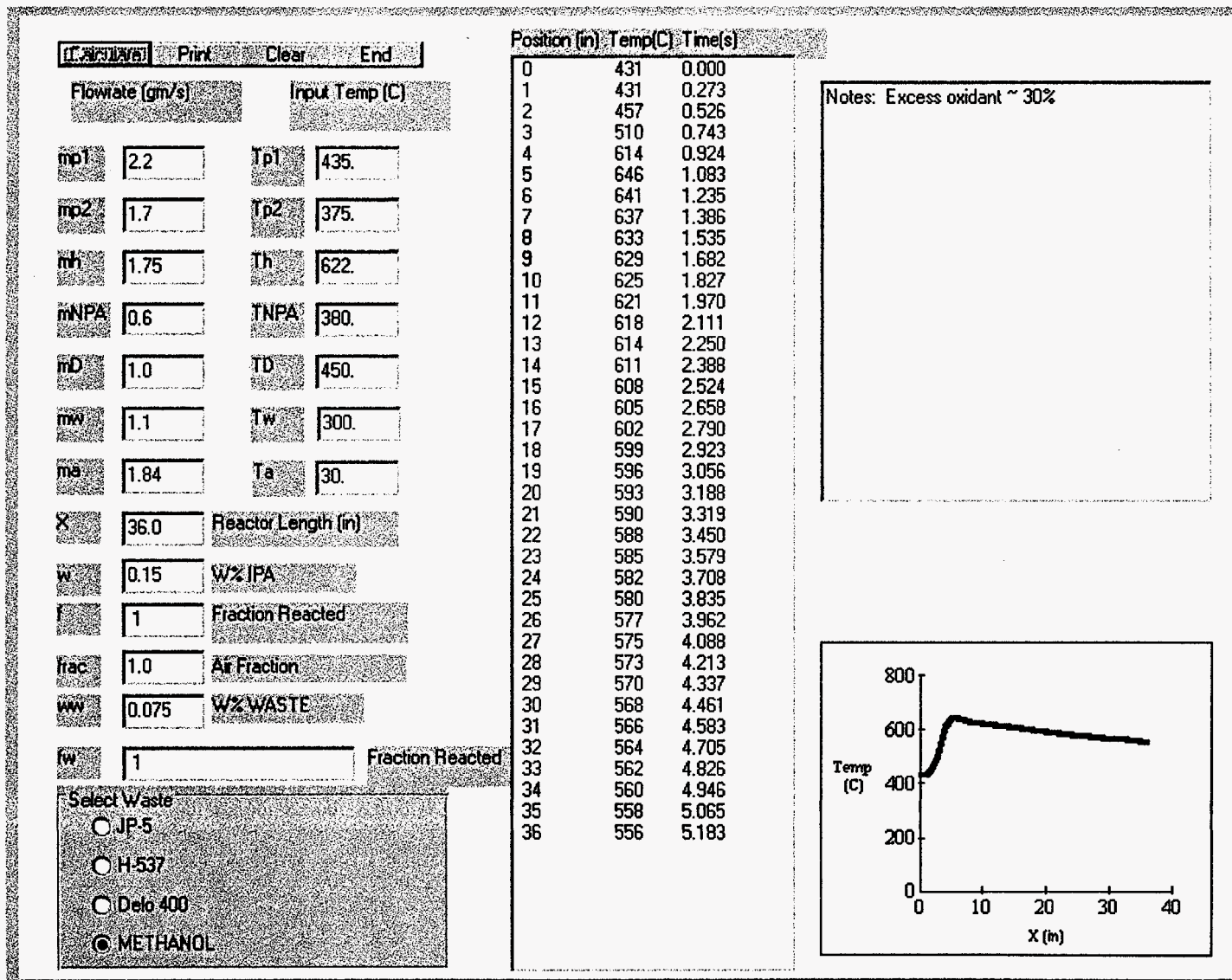


Figure 14. GUI for code. The destruction of methanol in the EER is modeled in the figure.

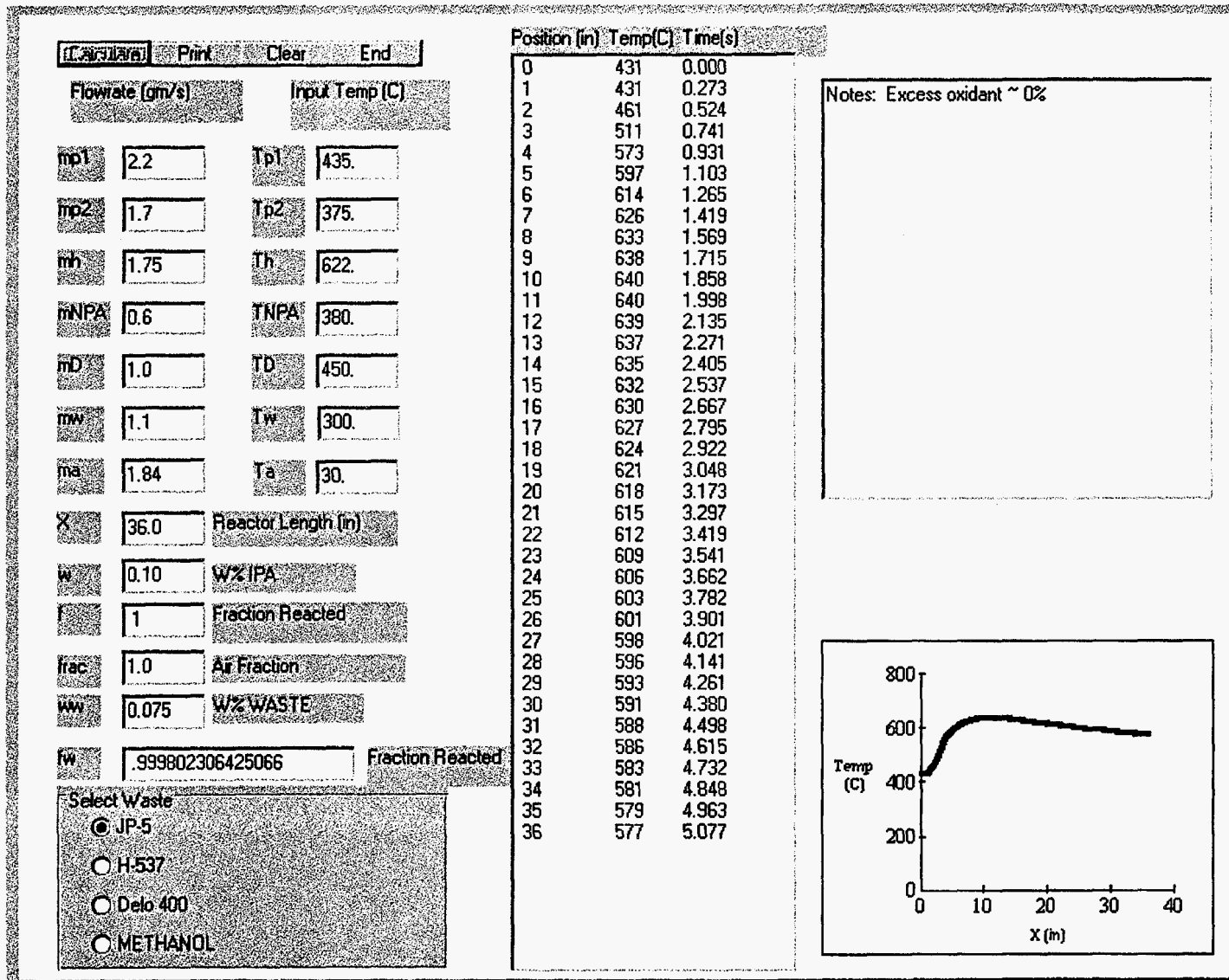


Figure 15. Calculated temperature profile, DRE, and residence time for the destruction of JP-5 (Input conditions from Table 5).

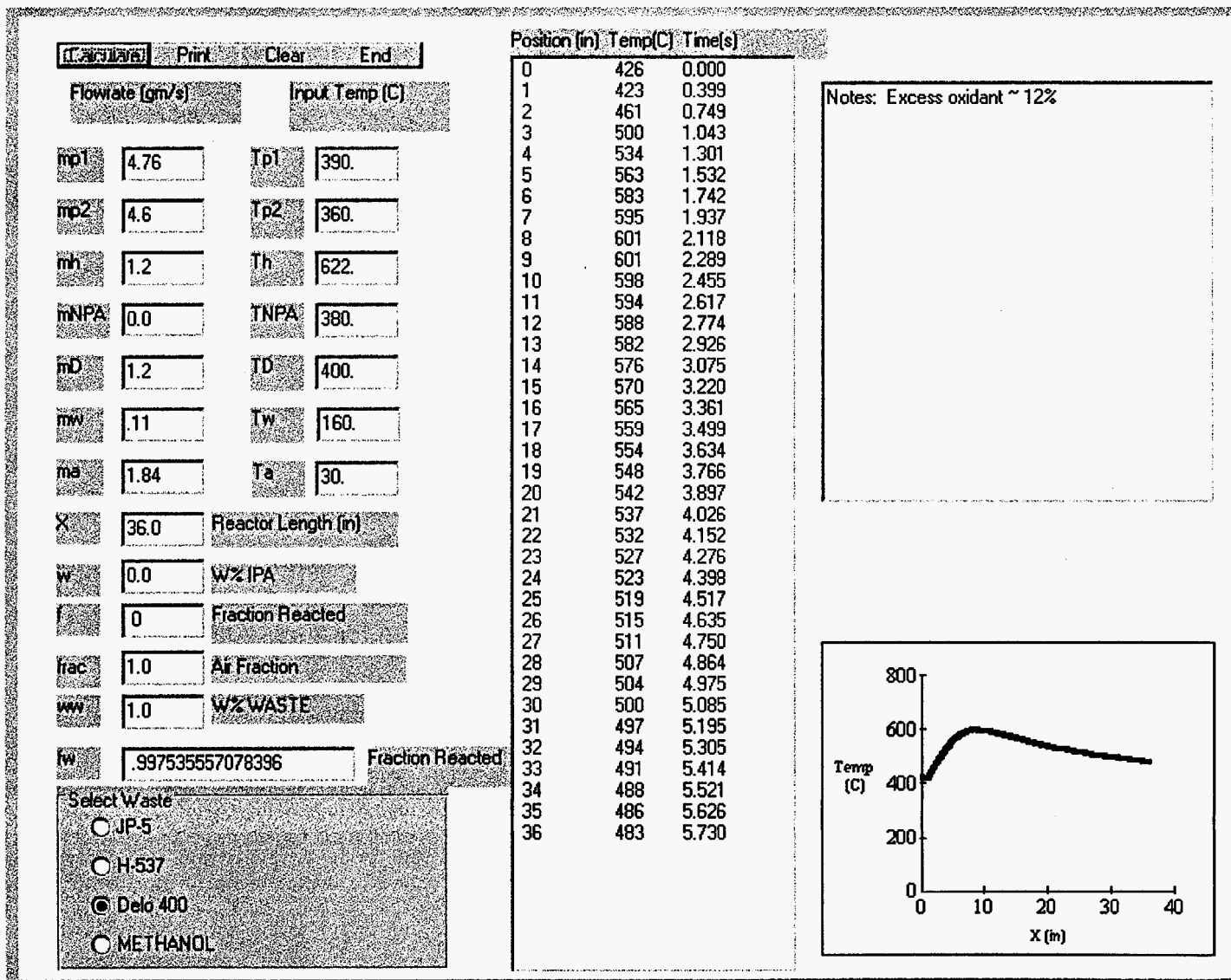


Figure 16. Calculated temperature profile, DRE, and residence time for the destruction of Oil (Input conditions from Table 9).

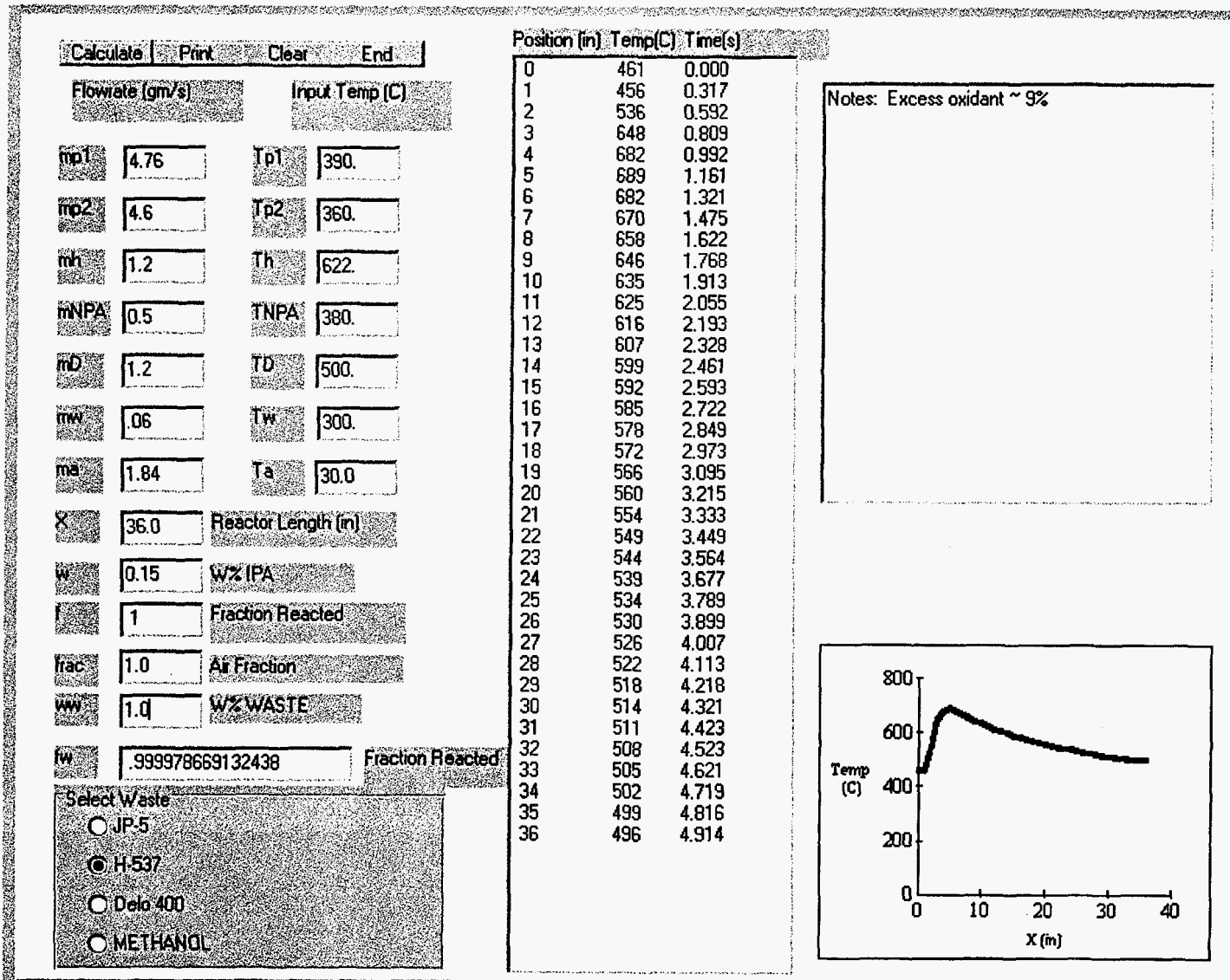


Figure 17. Calculated temperature profile, DRE, and residence time for destruction of Hydraulic Fluid (Input conditions from Table 11).

Appendix A. Code

Option Explicit
 Dim h(21), t(21), d(21) As Double
 Dim FLAG As Integer

Private Sub cmdCalc_Click()

'Code Inj: Begun April 5 1996

'Programmer and Modeler: Costanzo A. LaJeunesse June 28 1996

'Modified July 12 include two platelet sections

'Program models the temperature profile and reaction of several wastes using
 'NPA as the fuel for a SCWO reactor with transpiration boundary layer.
 'Code has model for heat release that is assumed to be one step of the form

$$d[\text{waste}]/dt = -k_{\text{eff}}[\text{waste}]$$

'k_{eff} equations based on TOC and may over estimate rate of heat release due
 'to rate of conversion of CO to CO₂ is not accounted for

'a = area of reactor [m²], diameter=1.1"
 'delx = 1 inch converted to [m], x=1"
 'cpa = specific heat of air [J/gm]
 'lamda = energy released by NPA [J/gm]
 'lamdaw = energy released by waste [J/gm]
 'w = weight percent - should be input as decimal fraction NPA
 'ww = weight percent - should be input as decimal fraction WASTE
 'f = fraction of NPA reacted
 'fw = fraction of waste reacted
 'frac = a value of frac > 1 can be used to calculate at x = 0
 ' theoretical three stream: mh,mipa,ha, where
 ' frac is the fraction of the air that mixes with the fuel.
 'mp = total platelet massflowrate (gm/s)
 'mh = heating or hot water massflowrate (gm/s)
 'mipa = stream holding ipa or npa total flowrate (gm/s)
 'md = diluent water flowrate (gm/s)
 'mw = waste flowrate (gm/s)
 'ma = air flowrate (gm/s)
 'T"i" = associate stream temp in (C)

Dim cpa, lamda, lamdaw As Double
 Dim mp1, mp2, mh, mipa, md, mw, ma As Double
 Dim tp1, tp2, th, tipa, td, tw, ta As Double

Dim delx, w, ww, f, fw, frac, a As Double

'hlhs = total enthalpy of fluid streams before thermodynamic equilibration
'temp = equilibrium temp in deg C.
'h,i = associated stream enthalpies
'mwtotal= total water flowrate [gm/s]
'x = stream location from top of injector [in]
'k = counter
'toprint= string variable

Dim hlhs, temp As Double
Dim hp1, hp2, hh, hipa, hd, hw, ha, mwtotal As Double
Dim k As Integer
Dim toprint As String
Dim x As Double

'these variables are returned from a subroutine to calculate
'residence time rt [s] and incremental time delt from x to x+1 [s]

Dim rt As Double
Dim delt As Double

,

'graph1 assignments (nonportable)

graph1.AutoInc = 0
graph1.NumSets = 1
graph1.ThisSet = 1
graph1.NumPoints = 37

'Read in input:

Call Readin(a, delx, cpa, lamda, lamdaw, w, ww, f, fw, frac, mp1, tp1, mp2, tp2, mh, th, mipa, tipa, md, td, mw, tw, ma, ta)

'find enthalpy in [J/gm] of all input streams:

Call enthalpy(hp1, tp1)
Call enthalpy(hp2, tp2)
Call enthalpy(hh, th)
Call enthalpy(hipa, tipa)
Call enthalpy(hd, td)
Call enthalpy(hw, tw)
ha = frac * cpa * ta

'beginning first increment forward from x=0 to x=1". Assume no instant reaction so set f=0 and fw = 0:

f = 0#
fw = 0#
x = 0#

k = 0

```
*****  
'Can release all the NPA at x = 0 by hardcoding f=1 here  
'f = 1#  
*****
```

Do

```
'hlhs = enthalpy lefthandside into location at x inches  
'find equilibrium temp, mwtotal is total water flowrate at location x  
'call to EqATX determines equilibrium temp a location x
```

```
  If (x <= 18#) Then  
    hlhs = x / 18# * mp1 * hp1  
    mwtotal = mh + mipa + x / 18# * mp1 + md + mw  
  End If
```

```
  If (x > 18#) Then  
    hlhs = mp1 * hp1 + (x - 18#) / 18# * mp2 * hp2  
    mwtotal = mh + mipa + mp1 + (x - 18#) / 18# * mp2 + md + mw  
  End If
```

```
  hlhs = hlhs + mh * hh + mipa * (hipa + f * w * lamda) + md * hd + mw * (hw + fw * ww * lamdaw)  
  + ma * ha
```

```
  Call eq_temp_at_x(hlhs, mwtotal, ma, frac, cpa, temp)
```

```
'Hold quantities to put in listbox in variable toprint
```

```
  toprint = Str(x) + " " + Str(temp)
```

```
'Find residence time rt and increment from last rt call
```

```
  Call res_time_at_x(temp, ma, mwtotal, a, k, delx, rt, delt)
```

```
'calculate heat release: returns f. fw the integrated amount of energy release to x from NPA and waste:
```

```
  If (w > 0#) Then Call heat_release_at_x(k, temp, delt, f)  
  If (ww > 0#) Then Call heat_releasew_at_x(k, temp, delt, fw)
```

```
*****  
'note use of f=1 if want all NPA reacted at x=0  
'f = 1#  
*****
```

```
'graphics output, increment x , and repeat:
```

```
  graph1.ThisPoint = k + 1  
  graph1.XPosData = x  
  graph1.GraphData = temp  
  x = x + 1#  
  k = k + 1  
  toprint = toprint + " " + Str(rt)  
  lstRes.AddItem toprint
```



```
20 Loop Until x > 36#
graph1.DrawMode = 2
txtf.Text = Str(f)
txtfw.Text = Str(fw)
End Sub
```

```
Private Sub cmdClear_Click()
lstRes.Clear
End Sub
```

```
Private Sub cmdEnd_Click()
End
End Sub
```

```
Private Sub cmdPrint_Click()
PrintForm
End Sub
```

```
Public Sub enthalpy(hr, ti)
'use linear interpolation
Dim i As Integer

Do
i = i + 1
If ti > t(i) Then
hr = h(i + 1) - ((h(i + 1) - h(i)) / (t(i + 1) - t(i)) * (t(i + 1) - ti))
Exit Sub
End If

Loop Until i = 21
```

```
End Sub
```

```
Private Sub Form_Load()
```

```
'Enthalpy, temperature, and density of water at 240 bar is hardcoded here
'Temperatures above 650C are not valid unless these arrays are increased.
```

```
h(1) = 24.04
h(2) = 229.92
h(3) = 437.1
h(4) = 647.2
h(5) = 862.3
h(6) = 1086.2
h(7) = 1330.9
```

$$h(8) = 1626.9$$

$$\begin{aligned}h(9) &= 1802\# \\h(10) &= 1872\# \\h(11) &= 2023\# \\h(12) &= 2373\# \\h(13) &= 2497\# \\h(14) &= 2577\#\end{aligned}$$

$$\begin{aligned}h(15) &= 2637.5 \\h(16) &= 2974\# \\h(17) &= 3179.7 \\h(18) &= 3348.2 \\h(19) &= 3499.8 \\h(20) &= 3642.15 \\h(21) &= 3779.5\end{aligned}$$

$$\begin{aligned}t(1) &= 0\# \\t(2) &= 50\# \\t(3) &= 100\# \\t(4) &= 150\# \\t(5) &= 200\# \\t(6) &= 250\# \\t(7) &= 300\# \\t(8) &= 350\#\end{aligned}$$

$$\begin{aligned}t(9) &= 370\# \\t(10) &= 375\# \\t(11) &= 380\# \\t(12) &= 385\# \\t(13) &= 390\# \\t(14) &= 395\#\end{aligned}$$

$$\begin{aligned}t(15) &= 400\# \\t(16) &= 450\# \\t(17) &= 500\# \\t(18) &= 550\# \\t(19) &= 600\# \\t(20) &= 650\# \\t(21) &= 700\#\end{aligned}$$

'density of water in kg/m³

$$\begin{aligned}d(1) &= 1011\# \\d(2) &= 998\# \\d(3) &= 969\# \\d(4) &= 930\# \\d(5) &= 881\# \\d(6) &= 821\# \\d(7) &= 742\# \\d(8) &= 621\#\end{aligned}$$

$$\begin{aligned}d(9) &= 528\# \\d(10) &= 485\# \\d(11) &= 384\#\end{aligned}$$

```
d(12) = 214#
d(13) = 179#
d(14) = 161#
```

```
d(15) = 149#
d(16) = 102#
d(17) = 85#
d(18) = 75#
d(19) = 68#
d(20) = 62#
d(21) = 58#
```

```
End Sub
```

```
Public Sub density(ti, rhoa, rhow)
Dim i As Integer
'use linear interpolation
```

```
i = 0
Do
i = i + 1
If t(i) > ti Then
rho = d(i + 1) - ((d(i + 1) - d(i)) / (t(i + 1) - t(i))) * (t(i + 1) - ti)
rhoa = 3500# * 6895# / 286# / (ti + 273#)
rhow = rhow * 1000#
rhoa = rhoa * 1000#
Exit Sub
End If
```

```
Loop Until i = 20
```

```
rhoa = 3500# * 6895# / 286# / (ti + 273#)
```

```
rhow = d(21) * 1000#
rhoa = rhoa * 1000#
End Sub
```

```
Private Sub Readin(a, delx, cpa, lamda, lamdaw, w, ww, f, fw, frac, mp1, tp1, mp2, tp2, mh, th, mipa,
tipa, md, td, mw, tw, ma, ta)
```

```
'a = area of reactor [m^2], diameter=1.1"
'delx = 1 inch converted to [m], x=1"
'cpa = specific heat of air [J/gm]
'lamda = energy released by NPA [J/gm]
'lamdaw = energy released by waste [j/gm]
```

```
a = (3.1417 / 4#) * (1.1 * 1.1) * 2.54 * 2.54 / 100# / 100#
delx = 1# * 2.54 / 100#
cpa = 1#
lamda = 33161#
```

```
'jp5,h537,delo400,methanol
If (FLAG = 0) Then lamdaw = 44000#
If (FLAG = 1) Then lamdaw = 44000#
If (FLAG = 2) Then lamdaw = 44000#
If (FLAG = 3) Then lamdaw = 22700#
```

```
'w = weight percent of NPA
'ww = weight percent of waste
'f = fraction of NPA reacted
'fw = fraction of waste reacted
'frac = a value of frac < 1 can be used to calculate at x = 0 theoretical three stream: mh,mipa,ha, where
' frac is the fraction of the air that mixes with the fuel.
```

```
w = Val(txtW.Text)
ww = Val(txtWW.Text)
f = Val(txtf.Text)
fw = Val(txtfw.Text)
frac = Val(txtfrac.Text)
```

```
'convert values from string to double, all are mass flowrates in gm/s: platelet,hot water,ipa,diluent or water
'protection circuit, waste, a, and associated input temperatures
```

```
mp1 = Val(txtMp1.Text)
mp2 = Val(txtMp2.Text)
mh = Val(txtMh.Text)
mipa = Val(txtMipa.Text)
md = Val(txtMd.Text)
mw = Val(txtMw.Text)
ma = Val(txtMa.Text)
tp1 = Val(txtTp1.Text)
tp2 = Val(txtTp2.Text)
th = Val(txtTh.Text)
tipa = Val(txtTipa.Text)
td = Val(txtTd.Text)
tw = Val(txtTw.Text)
ta = Val(txtTa.Text)
```

```
End Sub
```

```
Private Sub eq_temp_at_x(hlhs, mwtotal, ma, frac, cpa, temp)
```

```
Dim i, j As Integer
Dim delt As Double
Dim hrhs, hwrhs As Double
'counters i,j, temp = temperature [C], delt = temp increment [C]
i = 0
j = 0
temp = 0
delt = 50#
```

```
Do
```

```

'call for rhs enthalpy looking for equilibrium temp. Assume a temp and find associated enthalpy for
'the water, hwrhs, Add in the air portion to find the total enthalpy hrs
Call enthalpy(hwrhs, temp)
hrhs = mwtotal * hwrhs + ma * frac * cpa * temp

'hrhs is a monotoically increasing function, as soon as hrhs is bigger resolve to smaller temp
increment
If hrhs > hlhs Then
  delt = 50# / 50#
  temp = temp - 50#

  Do
    Call enthalpy(hwrhs, temp)
    hrhs = mwtotal * hwrhs + ma * frac * cpa * temp
    If hrhs > hlhs Then Exit Sub
    temp = temp + delt
    j = j + 1
  Loop Until j = 50

End If

temp = temp + delt
i = i + 1
Loop Until i = 21

End Sub

Private Sub res_time_at_x(temp, ma, mwtotal, a, k, delx, rt, delt)

' v = velocity vector [m/s]
' alpha = traditional void factor used in air water mixtures - definition only for this
' phenomenological model

Static v(1000) As Double
Dim alpha, rho, rhoa, rhow, mtotal, vave As Double

'Find Local Density, alpha is void fraction, rho is density, v is velocity, looking for residence
'time rt

  Call density(temp, rhoa, rhow)
alpha = 0
alpha = (ma / rhoa) / (ma / rhoa + mwtotal / rhow)
rho = alpha * rhoa + (1# - alpha) * rhow
mtotal = mwtotal + ma

'density function returns rho in gm/m^3. mtotal is in gm/s so velocity is in m/s units. Dividing delx
[m]
'by velocity v gives rt, the residence time in seconds
v(k) = mtotal / a / rho

If (k = 0) Then
  vave = v(k)

```

```

    delt = 0
    rt = 0
Else
    vave = (v(k) + v(k - 1)) / 2#
    delt = delx / vave
    rt = rt + delt
End If

End Sub

Private Sub heat_release_at_x(k, temp, delt, f)
' fn = fraction of NPA converted over delx at location k
' keff = rate constant as a function of temp
Static fn(1000) As Double
Dim sum As Double
Dim count As Integer
Dim keff As Double

'
If (k = 1) Then
' for short term kinetics
keff = Exp(-47181# / (temp + 273#) + 66.4)
' for long term kinetics
keff = Exp(-22000# / (temp + 273#) + 30.72)
fn(k) = 1# - Exp(-keff * delt)
f = fn(k)
End If

If k > 1 Then
'
keff = Exp(-47181# / (temp + 273#) + 66.4)
keff = Exp(-22000# / (temp + 273#) + 30.72)
fn(k) = 1# - Exp(-keff * delt)
count = k
sum = 1# - fn(k)

Do

sum = sum * (1 - fn(count - 1))
count = count - 1

Loop Until count = 1

f = 1# - sum
End If

If f > 1# Then f = 1#

End Sub

Private Sub heat_releasew_at_x(k, temp, delt, fw)
' fn = fraction of WASTE converted over delx at location k
' keff = rate constant as a function of temp
Static fn(1000) As Double
Dim sum As Double
Dim count As Integer
Dim keff As Double

```

```

If (FLAG = 0) Then keff = Exp(-5750# / (temp + 273#) + 7.125)
'H-537
If (FLAG = 1) Then keff = Exp(-18860# / (temp + 273#) + 21.4)
'Delo 400
If (FLAG = 2) Then keff = Exp(-5750# / (temp + 273#) + 7.125)
'Methanol
If (FLAG = 3) Then keff = Exp(-19460# / (temp + 273#) + 26.07)

'
If (k = 1) Then
' H-537
' keff = Exp(-18860# / (temp + 273#) + 21.4)
' JP-5
' keff = Exp(-5750# / (temp + 273#) + 7.125)
' fn(k) = 1# - Exp(-keff * delt)
' fw = fn(k)
End If

If k > 1 Then

' keff = Exp(-18860# / (temp + 273#) + 21.4)
' JP-5
' keff = Exp(-5750# / (temp + 273#) + 7.125)
' fn(k) = 1# - Exp(-keff * delt)
' count = k
' sum = 1# - fn(k)

Do

' sum = sum * (1 - fn(count - 1))
' count = count - 1

Loop Until count = 1

' fw = 1# - sum
End If

If fw > 1# Then fw = 1#

End Sub

Private Sub PanCal_Click()

End Sub

Private Sub SSOOption1_Click(Index As Integer, Value As Integer)

FLAG = Index

End Sub

```

UNLIMITED RELEASE
INITIAL DISTRIBUTION:

Phil Dell'Orco
Los Alamos National Laboratory
Mail Stop C920
Los Alamos, NM 87545

Jim Hurley
Armstrong Lab/EQC
Suite 2
Tyndall Air Force Base, FL 32403-5323

Richard Kirts
Naval Civil Engineering Laboratory
560 Laboratory Dr.
Port Hueneme, CA 93043-4328

Ray Goldstein
U.S. Army Armament Research Development
and Engineering Center
SMCAR-AES-P, Bldg 321
Picatinny Arsenal, NJ 07806-5000

Crane Robinson (10)
Armament Research, Development & Engineering
Center
SMCAR-AES-P, Building 321
Picatinny Arsenal, NJ 07806-5000

Mr. Dan Burch
Ordnance Engineering
Sea Department, Code 4022
Naval Surface Warfare Center
Crane, Indiana 47522

Allan Caplan
US Army EDEC
SCBRD-EN (Demil)
Bldg E4405, Room 216
Aberdeen Proving Ground, MD 21010-5401

Chuck Heyman
US Army EDEC
SCBRD-EN (Demil)
Bldg E4405, Room 216
Aberdeen Proving Ground, MD 21010-5401

Floyd Jennings
US Army EDEC
SCBRD-EN (Demil)
Bldg E4405, Room 216
Aberdeen Proving Ground, MD 21010-5401

Jerry Hawks
USADACS
Attn: SIOAC-TD
Savanna IL 61074-9639

James Q. Wheeler
Chief, Demil Technology Office
U.S. Army Defense Ammunition Center
and School
Attn: SMCAC-TD
Savanna, IL 61074-9639

Ed Ansell
Demil Technology Office
U.S. Army Defense Ammunition Center
and School
Attn: SMCAC-TD
Savanna, IL 61074-9639

Curtis Anderson
Chief, Energetics Systems Process Division
U.S. Army Armament Research
and Development & Engineering Center
SMCAR-AES-P, Bldg 321
Picatinny Arsenal, NJ 07806-5000

Dr. Alanna Mitchell
Walcoff
2001 North Beauregard Street, Suite 800
Alexandria, Virginia 22311

Jaffer Mohiuddin
Office of Technology Development
US Department of Energy
Trevion II, 12800 Middlebrook
Germantown, MD 20874

Dr. Peter Schmidt (5)
Program Officer
Physical Sciences Division & Materials Division
800 N. Quincy St.
Arlington, VA 22217-5660

Dr. Regina E. Dugan (5)
Science & Technology Division
Institute for Defense Analyses
1801 North Beauregard Street
Alexandria, VA 22311-1772

Commander
Pine Bluff Arsenal
Attn: SIOPB-ETD Loy Aikman
Pine Bluff, Arkansas 71602-9500

Commander
Pine Bluff Arsenal
Attn: SIOPB-ETD Jim Haley
Pine Bluff, Arkansas 71602-9500

Frank A. De Rosa
Glitsch Technology Corporation
1055 Parsippany Boulevard
Parsippany, NJ 07054

Michael Modell
Modell Environmental Corporation
23 Fresh Pond Place
Cambridge, MA 02139-4429

Mark M. Bianco, P.E.
Foster Wheeler Environmental Corporation
8 Peach Tree Hill Road
Livingston, New Jersey 07039

Prof. Earnest Gloyna
College of Engineering
University of Texas
Austin, TX 78712

Prof. Phillip A. Savage
Department of Chemical Engineering
3034 Dow Building
University of Michigan
Ann Arbor, MI 48109-2136

Prof. Jefferson W. Tester
Massachusetts Institute of Technology
Energy Laboratory
Room E40-455
77 Massachusetts Avenue
Cambridge, MA 02139

E. L. Daman
Foster Wheeler Development Corporation
12 Peach Tree Hill Road
Livingston, NJ 07039

K. S. Ahluwalia (5)
Foster Wheeler Development Corporation
12 Peach Tree Hill Road
Livingston, NJ 07039

Gopal Gupta
Foster Wheeler Development Corporation
12 Peach Tree Hill Road
Livingston, NJ 07039

Dr. David A. Hazlebeck
General Atomics
M/S 15-100D
350 General Atomics Court
San Diego, CA 92121-1194

Dr. Jeffrey Marqusee
ESTCP Program Manager
Office of the Under Secretary of Defense
Acquisition and Technology
3000 Defense Pentagon
Washington, DC 20301-3000

Dr. M. F. Young
GenCorp Aerojet
P.O. Box 13222
Sacramento, CA 95813-6000

Len Shoenman
GenCorp Aerojet
P.O. Box 13222
Sacramento, CA 95813-6000

Daniel Greisen
GenCorp Aerojet
P.O. Box 13222
Sacramento, CA 95813-6000

Don Rousar
GenCorp Aerojet
P.O. Box 13222
Sacramento, CA 95813-6000

John Beller
EG&G Idaho, Inc.
P.O. Box 1625
Idaho Falls, ID 83415-3710

Benjamin Wu
Molten Metal Technology
400-2 Totten Pond Road
Waltham, MA 02154

MS0861	T. Hitchcock 9103
MS0756	G. C. Allen, 6607
MS1143	J. F. Rice, 6600
MS9001	T. O. Hunter, 8000
	Attn: J. B. Wright, 2200
	M. E. John, 8100
	L. A. West, 8200
	W. J. McLean, 8300
	T. M. Dyer, 8700
MS9007	R. C. Wayne, 8400
MS9101	J. P. Damico, 8411
MS9101	P. T. Larson, 8413
MS9102	A. L. Hull, 8416
MS9108	E. T. Cull, 8414
MS9108	L. G. Hoffa, 8414
MS9105	B. G. Brown, 8412
MS9106	P. R. Bryson, 8417
MS9105	H. H. Hirano, 8419
MS9105	K. L. Tschritter, 8419
MS9221	T. T. Bramlette, 8422
MS9105	D.Y. Ariizumi, 8412
MS9105	J. P. Chan, 8412
MS9105	J. A. Lamph, 8412
MS9105	C. A. LaJeunesse, 8412
MS9105	T. N. Raber, 8412
MS9105	W. C. Replogle, 8419
MS9105	M. C. Stoddard, 8419 (10)
MS9105	B. L. Haroldsen, 8412 (10)
MS9042	B. Nilson, 8345
MS9042	S. Griffiths, 8345
MS9052	S. F. Rice, 8361 (10)
MS9403	T. J. Shepodd, 8713
MS9404	B. E. Mills, 8713
MS9404	J. F. C. Wang, 8713
MS9141	S. Johnston, 8103
MS9052	R. Hanush, 8361
MS9053	R. Steeper, 8352
MS9052	D. Hardesty, 8361
MS9103	K. Wally, 8111
MS9052	J. Aiken, 8361
MS9101	L. M. Mara, 8411
MS9221	D. A. Wright, 8421
MS9221	J. J. Bartel, 8418
MS9021	Technical Communications Department, 8815, for OSTI (10)
MS9021	Technical Communications Department, 8815/Technical Library, MS0899, 4414
MS0899	Technical Library, 4414 (4)
MS9018	Central Technical Files, 8950-2 (3)